Progress in Oceanography 176 (2019) 102140

Contents lists available at ScienceDirect

Progress in Oceanography

journal homepage: www.elsevier.com/locate/pocean

Transatlantic gradients in calcifying phytoplankton (coccolithophore) fluxes

Catarina V. Guerreiro[a,b,*], Karl-Heinz Baumann[b,c], Geert-Jan A. Brummer[d,e], Laura F. Korte[d], Carolina Sá[a,f], Jan-Berend W. Stuut[d,e]

[a] MARE, Marine and Environmental Science Centre, Faculdade de Ciências da Universidade de Lisboa, Campo Grande, 1749-016 Lisboa, Portugal
[b] University of Bremen, Geosciences Department, Klagenfurter Str. 2-4, 28359 Bremen, Germany
[c] University of Bremen, MARUM – Center for Marine and Environmental Sciences, Leobener Str. 8, 28359 Bremen, Germany
[d] NIOZ Royal Netherlands Institute for Sea Research, Department of Ocean Systems, and Utrecht University, Den Burg 1790 AB, the Netherlands
[e] Vrije Universiteit Amsterdam, Department of Earth Sciences, Faculty of Science, De Boelelaan 1085, 1081 HV Amsterdam, the Netherlands
[f] CIMA, Centre for Marine and Environmental Research, Universidade do Algarve, 8005-139 Faro, Portugal

A B S T R A C T

Tropical oceans provide a benchmark for future primary productivity in increasingly warmer, stratified and nutrient-depleted waters. In this context, we assess the export fluxes of calcifying phytoplankton (coccolithophores) across the tropical North Atlantic, from upwelling affected NW Africa, via three ocean sites along 12°N to the Caribbean. Sampling was undertaken by means of a spatial array of four time-series sediment traps collecting particle fluxes in two-week intervals, from October 2012 to February 2014, allowing to track temporal changes along the southern margin of the North Atlantic central gyre. Species composition and seasonal export fluxes of coccolithophores show steep gradients in two groups. Upper photic zone (UPZ) and placolith-bearing species dominated by *Emiliania huxleyi* and *Gephyrocapsa oceanica* are most abundant in the mesotrophic surface waters of the Cape Blanc upwelling system off NW Africa. They decline gradually towards the Caribbean, paralleled by increasing surface temperatures and decreasing surface chlorophyll-*a*. Meanwhile the abundance of lower photic zone (LPZ) species *Florisphaera profunda* and *Gladiolithus flabellatus* increase in the same direction, reaching fluxes up to 3–5 times higher in the western end of the transect compared to the UPZ flora in mesotrophic waters. Adapted to low light conditions, the LPZ species follow the geostrophic wind-forced deepening of the thermocline/nutricline westward in ever lower species diversity towards the Caribbean.

Temporal changes were marked by weak seasonality in coccolith fluxes at all four sites, modulated by latitudinal migration of the Intertropical Convergence Zone (ITCZ) at the tropical sites M1, M2 and M4, and by spatiotemporal variation in wind-forced upwelling at site CB. A seasonal mismatch was observed between LPZ and UPZ-oligotrophic taxa (i.e. *Umbellosphaera* spp., *Rhabdosphaera* spp.) vs. UPZ-opportunistic species (*E. huxleyi*, *G. oceanica*) at the western site M4 contrasting with the more similar seasonal patterns amongst all species towards site CB. We interpret this as reflecting the entire photic zone becoming increasingly nutrient enriched towards east whenever wind-forced mixing occurs due to the eastward shoaling of the thermocline/nutricline. Our synoptic observations of seasonally resolved export fluxes at four sites contribute to the spatiotemporal understanding of coccolithophore fluxes across the entire tropical North Atlantic, urging for considering phytoplankton- and carbonate production across the entire photic zone when projecting the effects of ocean warming on future primary production.

1. Introduction

Marine phytoplankton are at the base of most oceanic food-chains, accounting for about half of the global primary production, profoundly affecting global biogeochemical cycles and climate (e.g. Falkowski et al., 2008; Chavez et al., 2011; Thomas et al., 2012). The growth of marine phytoplankton varies regionally, depending on the prevailing atmospheric and upper-ocean dynamics. In tropical and subtropical open-ocean waters, phytoplankton production is strongly regulated by opposing gradients in light and nutrient availability, with the semi-permanent thermocline separating the nutrient-poor upper layer from the nutrient-enriched lower layer (Signorini et al., 2015; Poulton et al., 2017). Inside the ocean gyres, where a particularly deep (at 200–300 m water depth) and stable thermocline strongly limits primary production, nutrient supply occurs mostly via nitrogen fixation by diazotroph organisms (Chavez et al., 2011; Karl et al., 1997), the passage of storms (Rumyantseva et al., 2015) and diapycnal mixing along the stratified thermocline (e.g. Oschlies, 2002). Productivity increases towards the edges of the gyres, particularly on their eastern and equatorial boundaries, through the upwelling of cool and nutrient-rich waters and the discharge of nutrient-rich riverine waters (Dadou et al., 1996; McGillicuddy et al., 1998; Chavez et al., 2011). All these factors are, however, sensitive to climate change. Decreased overturning of surface waters by ocean warming and increased stratification would reduce the supply of nutrients to the photic zone (e.g. Behrenfeld et al., 2006; Polovina et al., 2008; Boyce et al., 2010; Lozier et al., 2011; Thomas

* Corresponding author at: MARE, Marine and Environmental Science Centre, Faculdade de Ciências da Universidade de Lisboa, Campo Grande, 1749-016 Lisboa, Portugal.
E-mail address: cataguerreiro@fc.ul.pt (C.V. Guerreiro).

https://doi.org/10.1016/j.pocean.2019.102140
Received 17 August 2018; Received in revised form 28 June 2019; Accepted 24 July 2019
Available online 24 July 2019
0079-6611/

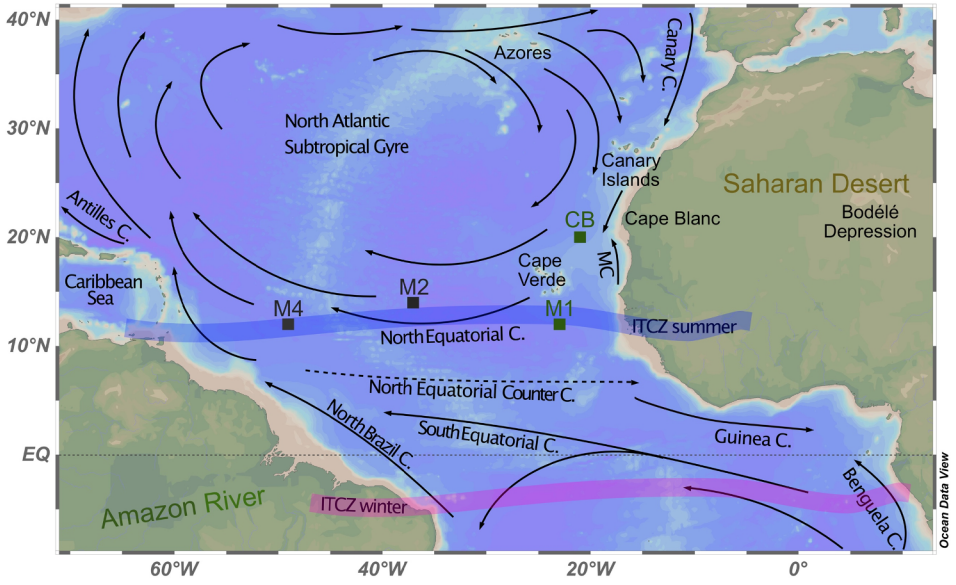

Fig. 1. Location of the sediment trap mooring sites (squares) and main surface currents (arrows) in the equatorial Atlantic Ocean, including the Mauritanian Current (MC) flowing northwards off NW Africa (adapted from Mann and Lazier, 2006; Pelegrí et al., 2017). New time-series from CB and M1 in the eastern tropical North Atlantic are indicated by green squares, with previously published data from M2 and M4 (Guerreiro et al., 2017) given in dark grey. Schematic representation of the seasonal migration of the Intertropical Convergence Zone according to Basha et al. (2015). (For interpretation of the references to colour in this figure legend, the reader is referred to the web version of this article.)

et al., 2012; Sunagawa et al., 2015; Moore et al., 2018) such that a decrease of phytoplankton production is likely to occur. Changes in phytoplankton species composition over the last 1000 years have been associated with increasingly warmer and more stratified water conditions, and to increasingly higher concentrations of atmospheric CO_2 (McMahon et al., 2015; Rivero-Calle et al., 2015). Some studies predict a poleward shift in species' thermal niches and a sharp decline in tropical phytoplankton diversity (e.g. Thomas et al., 2012), while others suggest that phytoplankton communities are able to adapt both physiologically and evolutionarily to climate change (Irwin et al., 2015).

Amongst the main marine phytoplankton groups, coccolithophores (Haptophyta) are the most important open-ocean primary producers covering their cells with tiny calcite plates (the coccoliths) (e.g. Rost and Riebesell, 2004). While they include species that successfully bloom in more dynamic and nutrient-enriched conditions (i.e. r-selected) (e.g. Knappertsbusch and Brummer, 1995; Guerreiro et al., 2013; O'Brien et al., 2016), coccolithophores as a group, are considered to be K-selected (Margalef, 1978; Brand, 1994), i.e. more typically occurring in the low-nutrient, stable and oligotrophic ocean (Brand, 1994; Winter et al., 1994; Boyd et al., 2010; O'Brien et al., 2016). A relative increase and expansion of coccolithophores towards higher latitudes has been reported to occur over the last decades in the Atlantic Ocean (Winter et al., 2014; Rivero-Calle et al., 2015). This poleward advance is consistent with the expansion of higher SSTs- and lower phytoplankton biomass (i.e. Chlorophyll-*a* concentration, Chl-*a*) in surface oceanic waters outside the equatorial upwelling (Polovina et al., 2008), suggesting gyre expansion by North Hemisphere warming. Such climate-induced ecological changes are likely to modify the patterns of primary production with cascading consequences for the pelagic food chain, as well as for the export of organic and inorganic carbon from the upper ocean to the deep-sea, which will feedback into the climate.

Coccolithophorid productivity is high and diverse in tropical North Atlantic phytoplankton. In the Cape Blanc upwelling region off NW Africa, upper photic zone (UPZ) species dominate, with high fluxes of *Emiliania huxleyi* and *Gephyrocapsa oceanica* (Köbrich and Baumann, 2009; Köbrich et al., 2015). However, in the central and western tropical North Atlantic, the lower photic zone (LPZ) coccolithophore species *G. flabellatus* and *F. profunda* dominate but also generate high coccolith export fluxes, while UPZ r-selected species occur intermittently, e.g. from short-term nutrient input by Amazon river discharge and Saharan dust deposition (Guerreiro et al., 2017). Living and sub-fossil coccolithophore assemblages indicate that differences in east-west species distribution in the equatorial Atlantic are associated with spatial gradients in thermocline and/or nutricline depth (Kinkel et al., 2000; Boeckel et al., 2006; Baumann et al., 2008). A possible cause for explaining such spatial gradient is the geostrophic deepening of the thermocline from the eastern to the western tropical North Atlantic, forced by combination of the NE trade winds with the Coriolis effect (Merle, 1980a,b; Katz, 1981).

Here, we document coccolith species fluxes from two new time-series sites in the eastern tropical Atlantic and integrate results with two others from sediment traps recently published from the central and western tropical Atlantic sampled the same year (Guerreiro et al., 2017). Combined, they form a transatlantic transect extending downstream and downwind from NW Africa (off Cape Blanc) to the Caribbean, adding up to a synoptic, synchronised and biweekly resolved record of coccolithophorid export productivity in the tropical North Atlantic. Coccolithophore fluxes are related to mass fluxes collected from the same sediment traps (Korte et al., 2017; Fischer et al., 2012, 2013, 2014) and to environmental parameters obtained from in situ Argo data, and with satellite remote sensing for the same year and at inter-annual time-scales for a broader and longer-term perspective.

2. Oceanographic and meteorological settings

The upper water masses in the study area, including the seasonal mixed layer, mostly consist of warm, salty and nutrient-depleted Tropical Surface Water (TSW) in the upper ~100 m (Temperature –T: ~27 °C, Salinity - S: 36.7–37) and cooler, less salty and relatively nutrient-enriched South Atlantic Central Water (SACW), at depths down to ~500 m (T: 6.0–18 °C, S: 34.3–35.8) (Emery and Meincke, 1986; Reid, 1994; Stramma and England, 1999). At the eastern part of the studied transect, SACW waters are found at < 100 m, shallow enough to reach the photic zone through the action of the surface winds, and with substantial contributions of the North Atlantic Central Water (NACW) in its lower part (300–550 m) (Pelegrí et al., 2017). Below, down to 1200 m water depth, the colder Antarctic Intermediate Water (AAIW) is characterised by a subsurface oxygen maximum and a salinity minimum (T: 2–6 °C, S: 33.8–34.8) (Emery and Meincke, 1986; Reid, 1994; Stramma and England, 1999) (see Figs. 2 and 3).

Surface water circulation, involving the TSW and the SACW, is mostly driven by the NE trade winds, generating the westward-flowing North Equatorial Current (NEC) between approximately 10°N and 20°N (Fig. 1). South of the NEC is the North Equatorial Counter Current (NECC) flowing in eastward direction, against the wind (Stramma and England, 1999). Both currents are subject to the latitudinal migration of

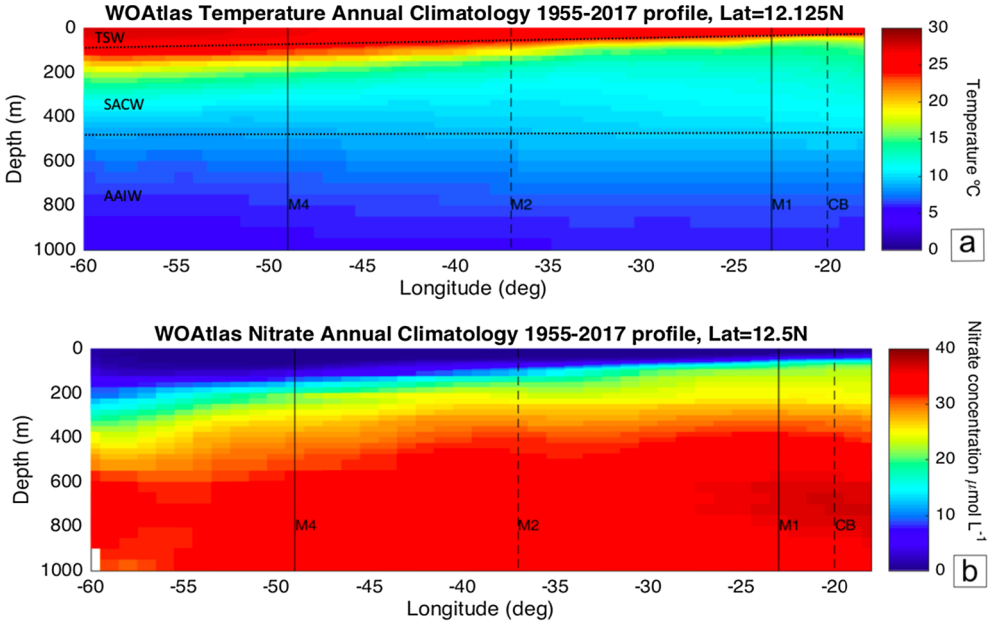

Fig. 2. Transatlantic depth profiles of temperature (a) and nitrate concentrations (b) along ~12°N, from 1955 to 2017 (World Ocean Atlas; Locarnini et al., 2013; Garcia et al., 2014, respectively). Main water masses (a) are the tropical surface water (TSW), South Atlantic Central Water (SACW) and Antarctic Intermediate Water (AAIW) based on Emery and Meincke (1986), Reid (1994), and Stramma and England (1999). Sediment trap moorings M2 (at 14°N) and CB (at 21°N) located north of 12°N are indicated by dashed vertical lines, whereas M4 and M1 (at 12°N) are indicated by solid vertical lines.

the Intertropical Convergence Zone (ITCZ), between approximately 5°S and 12°N, depending on the season (Basha et al., 2015). During boreal summer, when the ITCZ is at its northernmost position, the SE trade winds intensify along the equator, which intensify the ocean's surface circulation along the equator. Between summer and late fall, the NECC flows along an equatorial band centred between 5°N and 8°N (Longhurst, 1993; Garzoli and Katz, 1983).

On the northeastern side of the studied transect, the most important features are the equatorward flowing Canary Current (CC) and the eastward flowing Guinea Current (GC), the first being responsible for bringing colder waters from the North Atlantic Current (NAC) along the Iberian Peninsula and the northwestern coast of Africa. At the latitude of Cape Blanc (~21°N), the CC detaches from the continental shelf and veers in a southwestern direction, feeding into the NEC. There the southward flowing CC meets the northward flowing Mauritanian Current (MC) and the so-called Cape Verde Frontal System (CVFS) is formed (Barton, 1987; Zenk et al., 1991; Pastor et al., 2012), which separates colder subtropical- from warmer tropical waters. The CVFS is a region of significant offshore water export (Pastor et al., 2008; Alonso-González et al., 2009), favouring the advection of cold- and nutrient- and filament-rich surface water driven by yearlong coastal upwelling off Cape Blanc. The so-called "Giant Cape Blanc Filament"

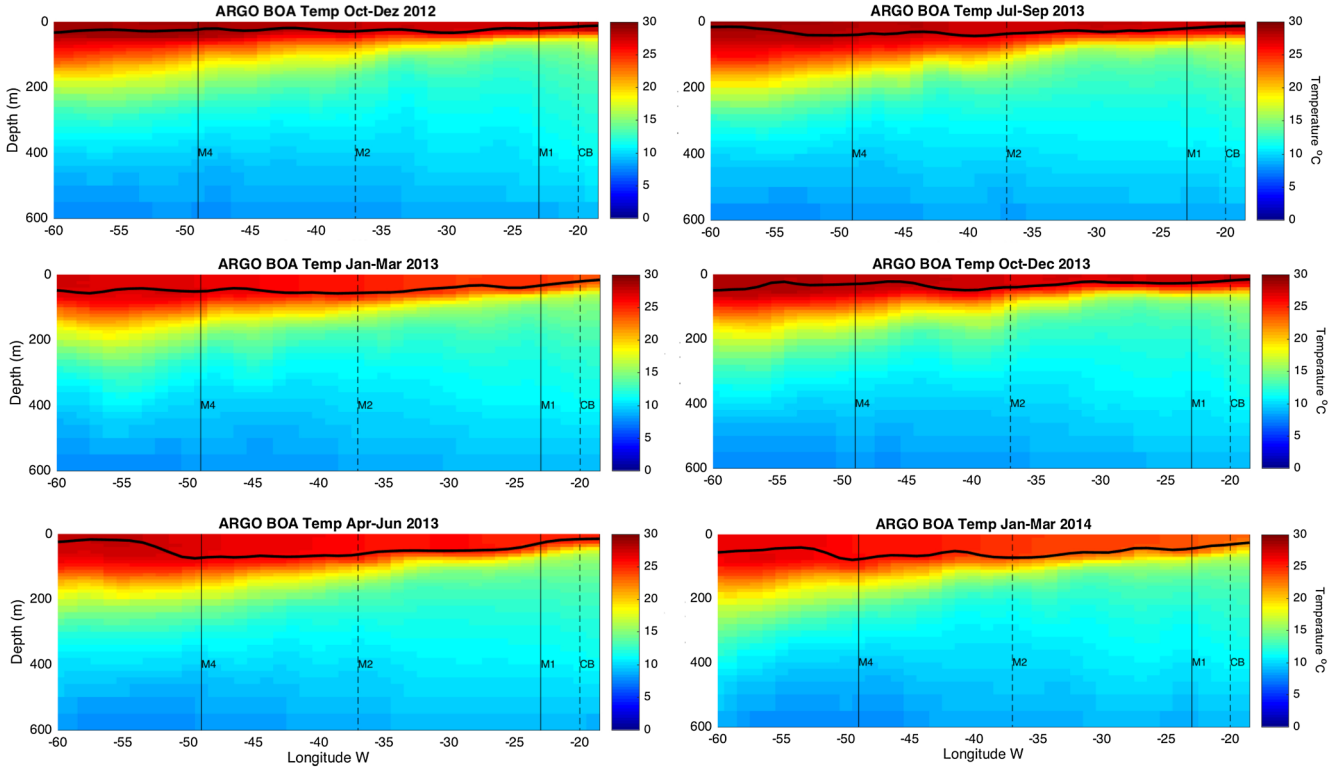

Fig. 3. Transatlantic depth profiles of temperature (°C) and mixed layer depth (MLD, black line) along ~12°N, from October 2012 to March 2014, obtained from in situ Argo-BOA data (Li et al., 2017; see Section 3.3).

(Van Camp et al., 1991; Gabric et al., 1993) is a permanent upwelling filament extending up to 600 km offshore where it interacts with the deep-ocean boundary (Gabric et al., 1993). South of the CVFS and closer to site M1, surface circulation is influenced by yearlong offshore upwelling associated with the Guinea Dome, a region of permanent, quasi-stationary cyclonic circulation (Pelegrí et al., 2017). The dome is part of the large-scale near-surface circulation associated with the NEC, the NECC and the North Equatorial Under Current (NEUC), acting to increase the height of the thermal ridge that extends zonally across the tropical North Atlantic (Siedler et al., 1992). When the ITCZ is displaced further south during winter-spring, the dome intensifies and moves onshore, whereas during summer-fall, when the ITCZ moves further north, the dome weakens and moves further offshore (McClain and Firestone, 1993; Pastor et al., 2013). The Cape Verde Basin is also located in the most prominent and persistent area of high aerosol input not only over the tropical Atlantic but world-wide, due to its proximity to the Saharan desert (e.g. Schuetz, 1980; Chiapello et al., 1999; Scheuvens et al., 2013).

On the western side of the transect, between summer and late fall, an important part of the northward flowing North Brazil Current (NBC) is retroflected off the South American northeastern margin towards the east into the western tropical North Atlantic after crossing the equator (Philander, 2001), feeding into the NECC (Richardson and Walsh, 1986). The retroflection of the NBC then forces the Amazon River plume to be displaced eastwards in the uppermost ~50 m of the water column (Boyle et al., 1977; De Master et al., 1986), carrying nutrient-rich waters far into the central equatorial North Atlantic (Muller-Karger et al., 1988; Ffield, 2005; Molleri et al., 2010; Varona et al., 2019). During boreal winter, the southward migration of the ITCZ causes the weakening of the trade winds along the equator and the ceasing of the NBC retroflection (Johns et al., 2004; Philander, 2001; Varona et al., 2019).

3. Material and methods

3.1. Sediment-trap sampling

Our study is based on new time-series from two sediment trap moorings in the eastern tropical North Atlantic (i.e., CB at 21°N 20°W and M1 at 12°N 23°W), which are combined with published flux data from two others in the central and western North Atlantic (M2 at 14°N 37°W and M4 at 12°N 49°W; Guerreiro et al., 2017). All sediment traps collected sinking particles during the same full year in a transatlantic transect extending from the mesotrophic region offshore Cape Blanc (NW Africa) into the Caribbean (Fig. 1, Table 1). Traps M1, M2 and M4 collected particles in synchronous intervals of 16 days, while trap CB collected particles at average intervals of 21 days. For details on mooring equipment, deployment/recovery of the traps and sample treatment, see Stuut et al. (2013) and Fisher et al. (2012, 2013, 2014). Temperature-pressure time-series recorded by in-situ sensors on the traps show that all four traps remained effectively vertical throughout deployment, while current velocity measurements remained well below the critical level of compromising collection efficiency (Korte et al., 2017; Fisher et al., 2012, 2013, 2014).

3.2. Laboratory and microscopic analysis

Sediment-trap samples from all stations were initially wet-sieved over a 1 mm mesh, wet-split into five aliquot subsamples using a rotary splitter (WSD-10, McLane Laboratories), washed to remove the $HgCl_2$ and salts, and centrifuged (detailed procedures in Korte et al. (2017) and Fischer et al. (2016)). For site CB, a 1/125 split of each original sample was used for coccolith analysis, without removing the organic material. For sites M1, M2 and M4, we used one 1/5 split of each original sample, after oxidation of organic matter in a low temperature Asher for approximately 4 h, to obtain a sample strictly composed of mineral particles (Fallet et al., 2009).

Coccolith export fluxes and species composition were assessed following Andruleit (1996) as detailed by (Guerreiro et al., 2017). Shortly, a split of usually 1/2000 to 1/2500 of the original sample was filtered onto polycarbonate membrane filters (47 mm diameter, 0.45 µm pore size). Once dried, a segment of each filter was cut and mounted on a Scanning Electron Microscope (SEM) stub. A minimum of 500 coccoliths was counted from an arbitrarily chosen transect across the filter and each coccolith was identified to the lowest taxonomic level possible at 3000× magnification, using a Zeiss DSM 940A SEM at 10 kV accelerating voltage. Species identification followed Jordan et al. (2004), Young et al. (2003) and Young et al. (2011). Coccolith counts were converted into fluxes (i.e. coccoliths/m^2/d) by extrapolating to the entire effective filter area and to the original sample and dividing by the sample interval and the trap aperture area. Finally, the Shannon-Weaver Diversity Index H′ (e.g. Tuomisto, 2013) was determined to assess species diversity through time at all four sites.

New coccolith flux of all the species data are presented for trap sites CB and M1. At sites M2 and M4, new coccolith flux data are presented for *Gephyrocapsa ericsonii*, *Calcidiscus leptoporus*, *Syracosphaera* spp. and *Calciosolenia* spp., whereas the fluxes of the other species have been recently published by Guerreiro et al. (2017). The latter results are figured (in grey) and described together with new coccolith fluxes from sites CB, M1, M2 and M4 (in green) to provide a basin-scale perspective on the distribution of each species/group of species. All data are shown oriented from west to east, upstream and up-wind along the southern margin of the North Atlantic central gyre. Given different depth habitats, we used the ratio between the UPZ species (*E. huxleyi* and *G.*

Table 1
Metadata and environmental information on sediment trap moorings M4, M2, M1 and CB.

Mooring station	M4	M2	M1	CB
Position	12°N 49°W	14°N 37°W	12°N 23°W	21°N 20°W
Environment	Tropical open-ocean seasonally Amazon-influenced	Tropical open-ocean	Tropical open-ocean near the Guinea Dome (yearlong offshore upwelling)	Tropical – Subtropical transition, yearlong influenced by coastal upwelling (NW Africa)
Trap depth (m)	1130	1235	1150	1214
Bottom depth (m)	4670	4790	5000	4160
Sampling period	19.10.2012–07.11.2013	19.10.2012–07.11.2013	19.10.2012–07.11.2013	CB-23: 04.10.2012–19.01.2013 CB-24: 24.01.2013–13.02.2014
Number of studied samples	23	23	24	22
Sampling resolution (days)	16	16	16	CB-23: 5 × 21,5 CB-24: 1 × 26 15 × 21 2 × 15,6

oceanica) and the LPZ species (*F. profunda* and *G. flabellatus*) to infer transatlantic variations in nutricline depth (Molfino and McIntyre, 1990; Stoll et al., 2007; Guerreiro et al., 2017).

3.3. Remote sensing and in situ Argo data

Time-series of meteorological and hydrological parameters were obtained from satellite remote sensing and in situ Argo databases. Sea surface temperature (SST) is used as a proxy for thermal stratification (Signorini et al., 2015), Mixed Layer Depth (MLD) and wind speed as indicators for seasonal wind-forced water mixing (i.e. ≫ wind speed, ≫ MLD), and sea surface Chl-*a* concentration for surface phytoplankton productivity. Daily precipitation and wind speed are also used as indicators for seasonal migration of the ITCZ across the tropical North Atlantic (i.e. ≫ precipitation and ≪ wind speed indicate a greater influence of the ITCZ; Oschlies and Garçon, 1998). Satellite data (datasets details provided in Supplementary Material) were retrieved for each trap location using a 2° × 2° latitude-longitude area around the trap location and averaged for each sediment trapping interval. The 2° × 2° box, corresponding to ~108 × 108 N mi (1° = ~59 N mi), was taken as representative of the catchment area of a trap deployed at 1200 m depth, given the sinking speed for marine phytoplankton and algal aggregates (e.g. Waniek et al., 2000). Remote-sensing data were downloaded from various sources as listed in the Supplementary Material and processed for the study period of 2012–2014 (Fig. 7a–c). For the long-term data, MODIS L3-annual 4-km composites SST – 11 µm night product for 15 years (i.e. 2003–2017) were downloaded and averaged to retrieve an annual SST climatology. Subtracted from the mean SST for the trap-sampling period (i.e. October 2012–November 2013) it yields a map of SST anomalies relative to the annual climatology shown in Fig. 11c. The annual SST climatology as well as the decadal temperature anomalies shown in Fig. 11e were also computed using the World Ocean Atlas data with 0.25° resolution (Locarnini et al., 2013) available from https://www.nodc.noaa.gov/OC5/woa13/. MLD in situ data shown in Fig. 3 and 7b were obtained by trimestral-averaging the monthly Global Ocean Argo gridded data set (BOA-Argo; Li et al., 2017; Shaolei et al., 2018) and from the Argo mixed-layer monthly-climatology (2000–2017) database (Holte et al., 2017; http://mixedlayer.ucsd.edu) respectively. MLD data shown in Fig. 7b were determined by averaging for the sampling periods the daily data obtained from the NASA Ocean Biogeochemical Model (NOBM) VR2017 (Gregg and Rousseaux, 2017).

4. Results

4.1. Total coccolith export fluxes and species diversity

Highest coccolith fluxes were found at both ends of the transatlantic transect (Fig. 4). From east to west, coccolith fluxes reached an annual mean of 79 × 10^7 coccoliths $m^{-2} d^{-1}$ at site CB and 54 × 10^7 coccoliths $m^{-2} d^{-1}$ at station M1, compared to 66 × 10^7 coccoliths $m^{-2} d^{-1}$ at site M2 and up to 3–5 times higher mean fluxes at the western tropical Atlantic, with 247 × 10^7 coccoliths $m^{-2} d^{-1}$ at site M4 (Table 2). Coccolith fluxes showed a low seasonality in all four locations, but particularly at sites M1 and M2. Comparatively higher seasonality offshore Cape Blanc showed a conspicuously different pattern from the other sites, with highest coccolith fluxes from late winter to early summer, and lowest during fall and early winter. (Fig. 4). Site M1 showed a weaker but similar seasonality compared to M2 and M4, with slightly higher fluxes during the fall of 2012 (October–November), spring (March and April) and summer (July and September) of 2013 (read Guerreiro et al., 2017 for a detailed coccolith flux and seasonal description of traps M2 and M4).

Site CB showed the highest number of coccolithophore taxa (58) and the highest Shannon–Weaver diversity index (annual mean H′ = 7.5, compared to 7.3 at M1, 3.3 at M2 and 3.8 at M4; see Fig. 4). Site M1 contained lower number of taxa (38) compared to M2 and M4 (43 and 45, respectively; Guerreiro et al., 2017) but showed a H′ similar to station CB. H′ was also seasonally more variable at the eastern sites M1 and CB compared to the central and western sites M2 and M4 (Fig. 4).

Total coccolith fluxes were positively correlated with total mass fluxes along the entire transect, particularly at sites CB and M2 (Fig. 5a–d). Shannon–Weaver diversity index was negatively correlated with total mass fluxes at both ends of the transect, and positively correlated at sites M1 and M2 (Fig. 5e–h).

Of the observed coccolithophore taxa, only 14 occurred in relative abundances > 3% in at least one of the studied traps on an annual basis, and these were selected for further analysis. Taxa displaying a similar basin-scale distribution were grouped together (Fig. 6). Mean, minimum, and maximum coccolith fluxes and percentages for each taxon or group of taxa are given in Table 2.

4.2. Coccolithophore species fluxes and relative abundances

The LPZ species *F. profunda* and *G. flabellatus* were dominant on a mean basin-scale, with 44 × 10^7 and 24 × 10^7 coccoliths $m^{-2} d^{-1}$, respectively, followed by the UPZ species *E. huxleyi* with 15 × 10^7 coccoliths $m^{-2} d^{-1}$ (Table 2). Other taxa, such as *Umbellosphaera* spp., *G. oceanica*, *Syracosphaera* spp., *Umbilicosphaera* spp., *Helicoshaera* spp., *G. muellerae* and *Rhabdopshaera* spp. produced mean fluxes of 2–5 × 10^7 coccoliths $m^{-2} d^{-1}$, whereas *G. ericsonii*, *Calcidiscus leptoporus*, *Reticulofenestra sessilis* and *Calciosolenia* spp. did not exceed 2 × 10^7 coccoliths $m^{-2} d^{-1}$. In terms of annual mean percentages, *F. profunda* (42%), *E. huxleyi* (16%) and *G. flabellatus* (12%) dominated export productivity, followed by *Umbellosphaera* spp., *G. oceanica*, *Helicosphaera* spp., *Umbilicosphaera* spp. and *Syracosphaer*a spp. with percentages of 3–5%, and the remaining taxa with 1–2%.

4.3. Spatial variations in coccolith species composition

Most of the taxa showed higher coccolith fluxes either at one or at

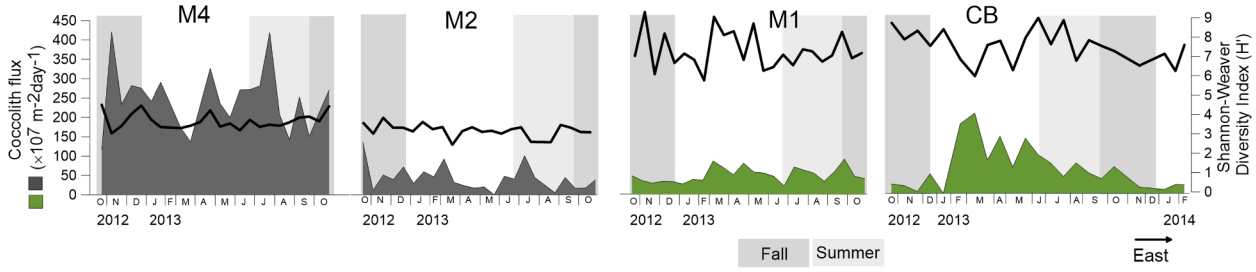

Fig. 4. Spatiotemporal variation in total coccolith export fluxes (coccolith $m^{-2} d^{-1}$; grey and green), and Shannon–Weaver diversity index (H′; black line), at trap sites M4, M2, M1 and CB. Published data from M2 and M4 (Guerreiro et al., 2017) are shown in grey. (For interpretation of the references to colour in this figure legend, the reader is referred to the web version of this article.)

Table 2
Annual mean and range of coccolith fluxes and relative abundances of the most abundant coccolithophore taxa (mean > 3%) for mooring sites M4, M2, M1 and CB. Species data marked with (*) for traps M4 and M2 are from Guerreiro et al. (2017).

Taxa	Coccolith fluxes (coccoliths $m^{-2} d^{-1} \times 10^7$)								Relative abundances (%)							
	M4		M2		M1		CB		M4		M2		M1		CB	
	Mean	Min-Max	Mean	Min-Max	Mean	Min-Max	Mean	Min-Max	Mean	Min-Max	Mean	Min-Max	Mean	Min-Max	Mean	Min-Max
Total fluxes	246	116–421	66	25–153	50	21–91	79	15–215								
UPZ TAXA																
C. leptoporus	1	0–3	1	0–1,4	1	0,1–1	3	0,4–12	0,2	0–1	1	0–2	1	0,4–3	4	2–8
Calciosolenia spp.	1	0–6	1	0–2	0,3	0–2	2	0,2–9	1	0–2	1	0,1–2	1	0–5	2	1–6
*E. huxleyi**	17	4–69	4	1–14	8	3–16	29	2–99	7	3–21	5	3–13	16	8–21	34	15–51
G. ericsonii	2	0–16	0,3	0–2	2	0,3–4	2	0,3–4	1	0–6	0,4	0–1	3	1–5	3	1–10
*G. muellerae**	7	0–72	0,2	0–1	0,3	0–1	1	0–2	3	0–25	0,3	0–1	1	0–2	2	0–11
*G. oceanica**	4	0,2–26	0,3	0–1	3	1–5	5	1–15	2	0,1–9	0,4	0–2	5	1–12	8	2–18
Helicosphaera spp.*	2	0,1–6	2	1–4	4	1–8	2	0,2–8	1	0,1–2	3	1–9	8	6–12	2	1–4
Rhabdosphaera spp.*	4	0–11	2	0,3–5	1	0–4	1	0,2–3	1	0–3	2	1–5	2	0–4	1	0–4
Syracosphaera spp.	4	1–13	2	0,3–5	1	0,2–4	4	0,3–15	2	1–4	2	1–5	2	0,4–4	4	2–8
Umbellosphaera spp.*	9	3–16	5	1–11	2	0,3–5	3	0,1–18	4	2–8	7	4–10	4	1,2–7	4	0,3–12
Umbilicosphaera spp.*	3	1–6	1	0,3–3	2	1–6	4	1–12	1	0,3–2	2	1–3	5	1–8	5	3–8
LPZ TAXA																
*F. profunda**	96	51–235	39	14–90	22	10–40	17	5–47	39	29–56	60	53–72	45	36–53	23	12–34
*G. flabellatus**	85	36–146	6	2–24	2	0,3–4	2	0,1–6	35	18–47	9	4–16	3	1–6	2	0,4–5
*R. sessilis**	2	1–5	2	0,4–3	1	1–2	0,3	0–1	1	0,2–2	3	1–4	3	1–6	0,4	0–1

both ends of the transatlantic transect, as often also reflected in their relative abundances. Two main groups of coccolithophore taxa stood out for showing a clear E-W distribution trend in terms of abundances. *Emiliania huxleyi*, *G. oceanica*, *Umbilicopshaera* spp., *C. leptoporus*, *Calciosolenia* spp. (Fig. 6b, d, g, h, k) and to some extent *Syracosphaera* spp. (Fig. 6i), generally decreased in abundance from east to west, particularly noticeable between CB and M2. By contrast, fluxes and abundances of *F. profunda* and *G. flabellatus* clearly increased westward (Fig. 6a). Of the latter, *F. profunda* was dominant further west and at the more open-ocean stations, with 45%, 60% and 39% of the annual mean assemblage at M1, M2 and M4, respectively. *G. flabellatus* attained 35% at M4, but dropped to only 9%, 3% and 2% at M2, M1 and CB, respectively. *E. huxleyi* was dominant at the northeastern end of the transect, with an annual mean of 34% at site CB, compared to only 8%, 5% and 7% at stations M1, M2 and M4, respectively (see Table 2).

Exceptions to these E-W trends include *Helicosphaera* spp. and *R. sessilis* which were more abundant at the central part of the transect, reaching their highest abundance at sites M1 and M2 (Fig. 6f and j). *G. muellerae* and *G. ericsonii* occurred in low abundance throughout the year at most of the sites but significantly increased at both ends of the basin, reaching together up to 21% and 32% at sites CB and M4, respectively (Fig. 6c). *Umbellosphaera* spp. and *Rhabdosphaera* spp. also

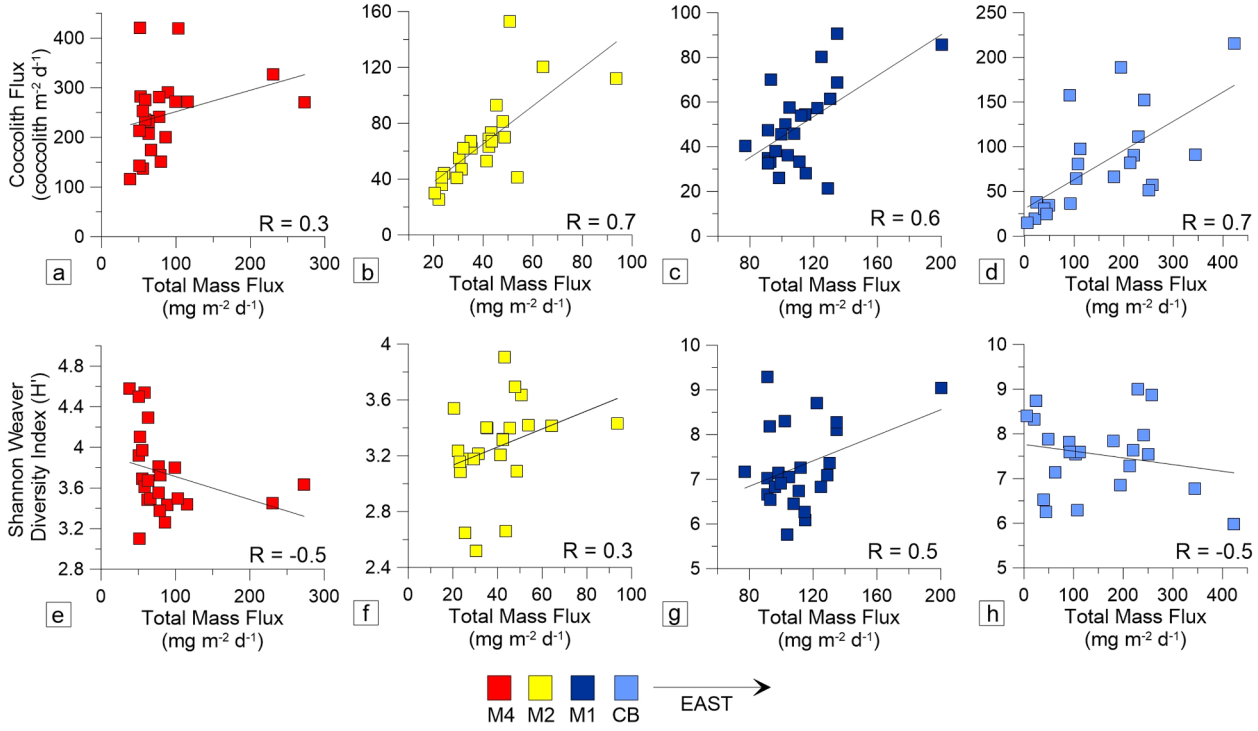

Fig. 5. Correlation of total coccolith fluxes and Shannon-Weaver diversity index (H′) with total mass fluxes at mooring sites M4, M2, M1 and CB. Total mass flux data from M1, M2 and M4 and total coccolith fluxes from M2 and M4 were recently published by Korte et al. (2017) and Guerreiro et al. (2017), respectively.

lacked any clear spatial trend, showing fairly similar mean percentages at all four locations but slightly more abundant at site M2 (Fig. 6e).

4.4. Seasonal patterns

Florisphaera profunda, *G. flabellatus*, *Umbellosphaera* spp., *Rhabdosphaera* spp. and *R. sessilis* were generally more abundant during summer and fall further west but increasingly more abundant during spring towards the northeast end (Fig. 6a, e, j). In contrast, *Syracosphaera* spp. and *Calciosolenia* spp. were most abundant during spring at both ends of the transect but increasing during fall at the more central stations (Fig. 6I and k). Usually *E. huxleyi* was more abundant during late winter and spring at all sites (Fig. 6b), whereas *Helicosphera* spp. (Fig. 6e) was more abundant from late winter to summer. *C. leptoporus* was clearly more abundant from late winter to early summer at site CB and showed two flux pulses in winter and summer at site M4 but showing a weak seasonality in the central part of the transect (Fig. 6h). None of the observed gephyrocapsid species revealed a clear seasonal pattern; *G. oceanica* was more abundant in spring but also increased during summer (at CB) and fall (at M4) (Fig. 6d), while *G. muellerae* and *G. ericsonii* mostly occurred in pulses during winter at both ends of the transect (Fig. 6c).

5. Discussion

Our study area is characterized by a wide range of meteorological and oceanographic processes (see Section 2) affecting primary production and the composition of coccolithophore communities by controlling nutrient availability in the photic zone, all of which are wind-forced and susceptible to climate change. Such interplay of factors is

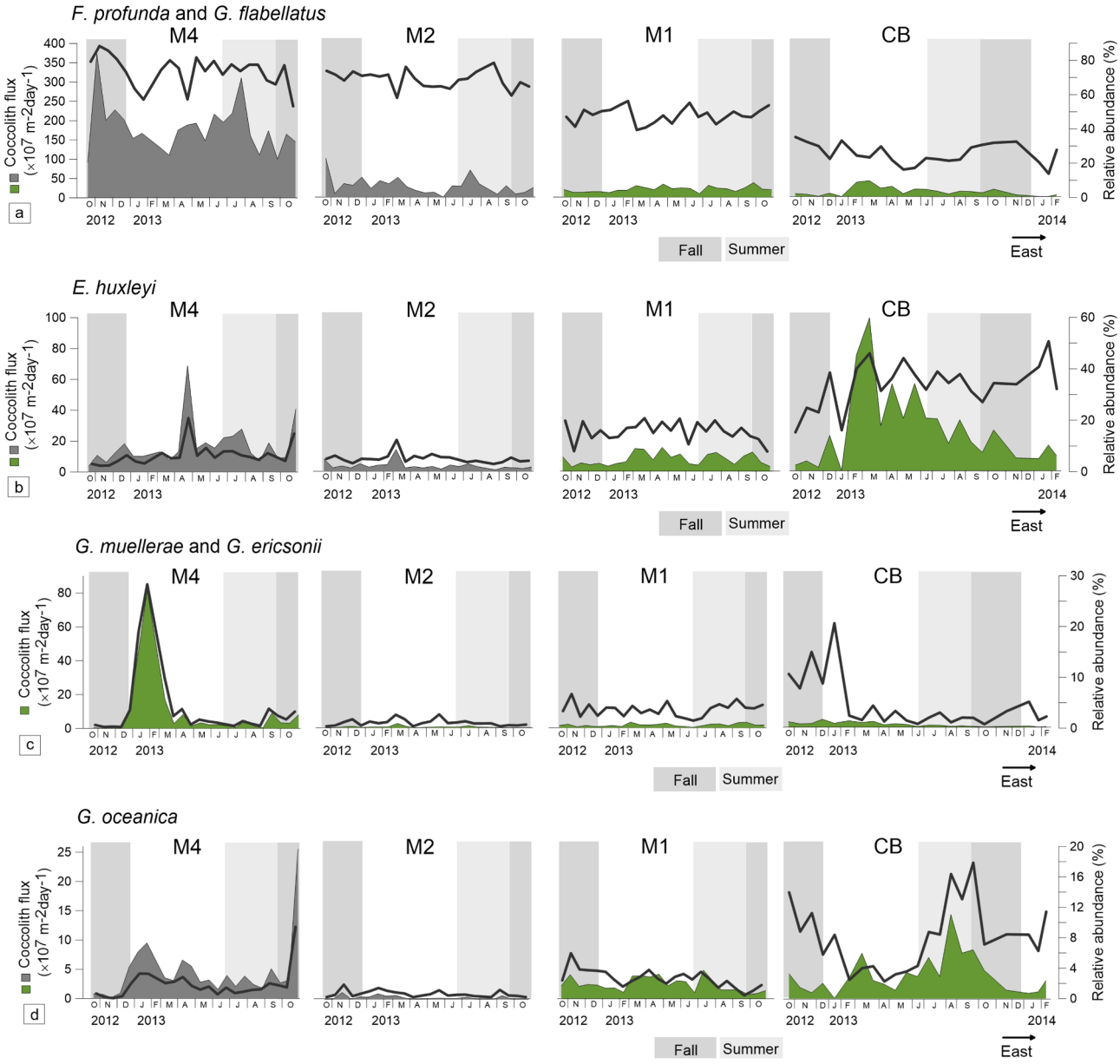

Fig. 6. Coccolith export fluxes (grey and green) and relative abundance (black line) of the most important species at (from east to west) sites M4, M2, M1 and CB: (a) *F. profunda* and *G. flabellatus,* (b) *E. huxleyi,* (c) *G. muellerae* and *G. ericsonii,* (d) *G. oceanica,* (e) *Umbellosphaera* spp. and *Rhabdosphaera* spp., (f) *Helicosphaera* spp., (g) *Umbilicosphaera* spp., (h) *C. leptoporus*, (i) *Syracosphaera* spp., (j) *R. sessilis* and (k) *Calciosolenia* spp. Dark and light grey thick bars indicate boreal fall and summer, respectively. Previously published data from M2 and M4 are shown in grey. (For interpretation of the references to colour in this figure legend, the reader is referred to the web version of this article.)

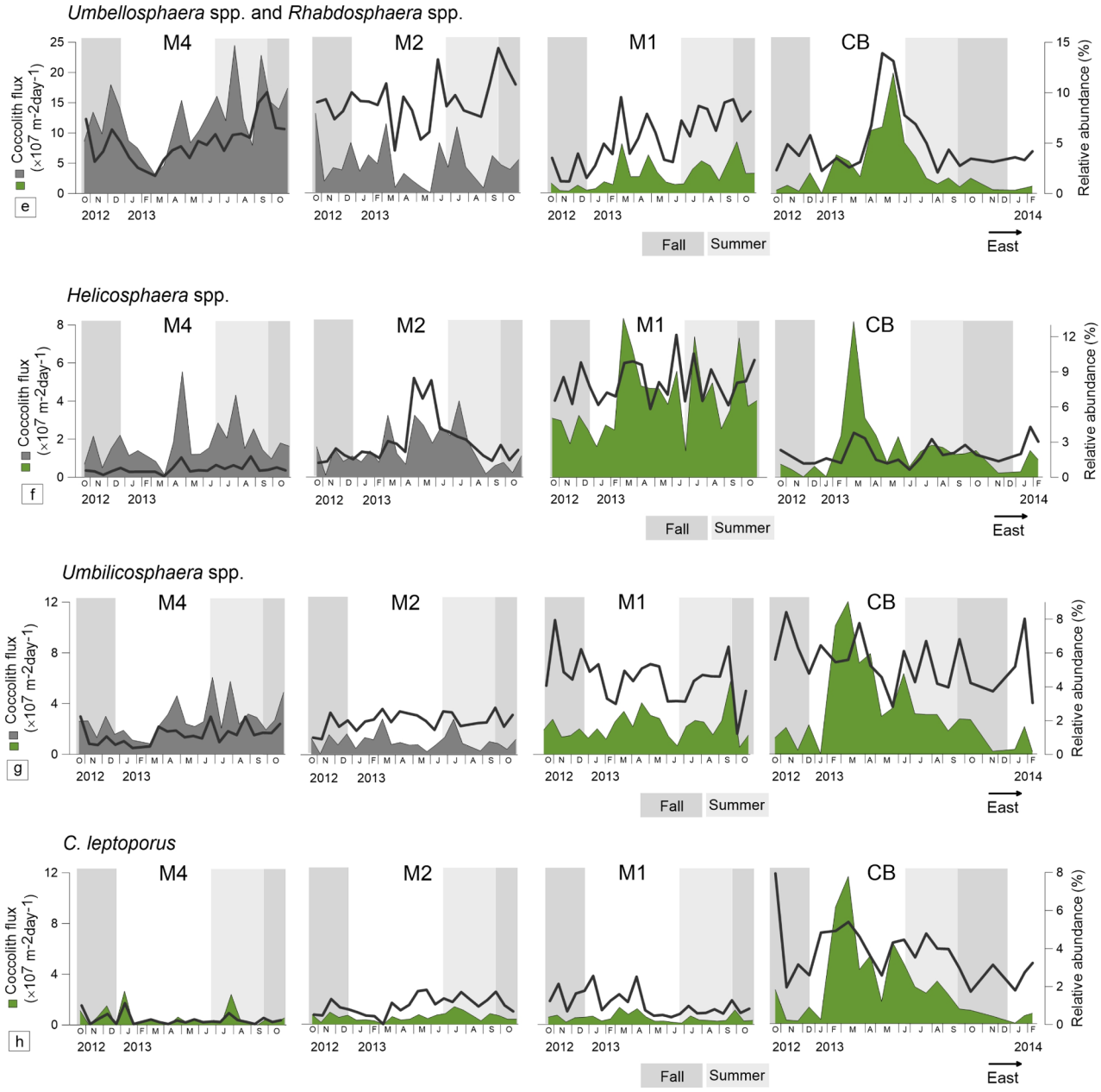

Fig. 6. (*continued*)

clearly reflected in strong linkages of our sediment trap time-series coccolith flux records to local hydrographic and climatic forcing prevailing in this area, as discussed in the following sections.

5.1. Spatiotemporal variability in coccolith export fluxes

5.1.1. Comparison between sites CB, M1, M2 and M4

Higher coccolith fluxes and slightly more pronounced seasonality at the easternmost (CB) and westernmost site (M4), suggests higher environmental variability at both ends of the transatlantic transect. We interpret this as probably resulting from the closer proximity of CB and M4 to the NW African and NE South American margins, respectively. Persistently stronger winds and much lower precipitation rates at site CB indicates a conspicuously different setting from the more open-ocean tropical sites M1, M2 and M4 (Fig. 7a). Lowest SST and much higher surface Chl-*a* concentrations are rooted in the strong and year-long coastal upwelling throughout the year (Fig. 7b), forced by persistent trade winds offshore Cape Blanc, combined with offshore wind-curl induced upwelling (Pastor et al. 2013). Strong upwelling during late winter coincides with maximum surface Chl-*a* in early February 2013, minimum SST and maximum seasonal MLD, following a period of enhanced wind strength (Fig. 7b).

High surface productivity at CB is evidenced by increased UPZ/LPZ ratios and of total coccolith fluxes (Fig. 7b and f), with highest occurrences of *E. huxleyi*, *Helicosphaera* spp. *Umbilicosphaera* spp., *C. leptoporus* and *Syracosphaera* spp. in February-March (Fig. 6b, f, g, h, i). This agrees with previous studies reporting highest surface Chl-*a* concentrations in late-winter to spring (Thomas et al., 2004), coinciding with the Cape Blanc "giant filament" reaching its largest offshore extension (Van Camp et al., 1991; Fischer et al., 2009a). The observed dominance of *E. huxleyi* and the highest abundances of *G. oceanica* at persistently high UPZ/LPZ ratios (Fig. 7b–d) reflect their opportunistic adaptation (Winter et al., 1994; Baumann et al., 2000; Andruleit, 2007; Boeckel and Baumann, 2008) to more dynamic and eutrophic environments (e.g. Kinkel et al., 2000; Guerreiro et al., 2013; Poulton et al., 2017).

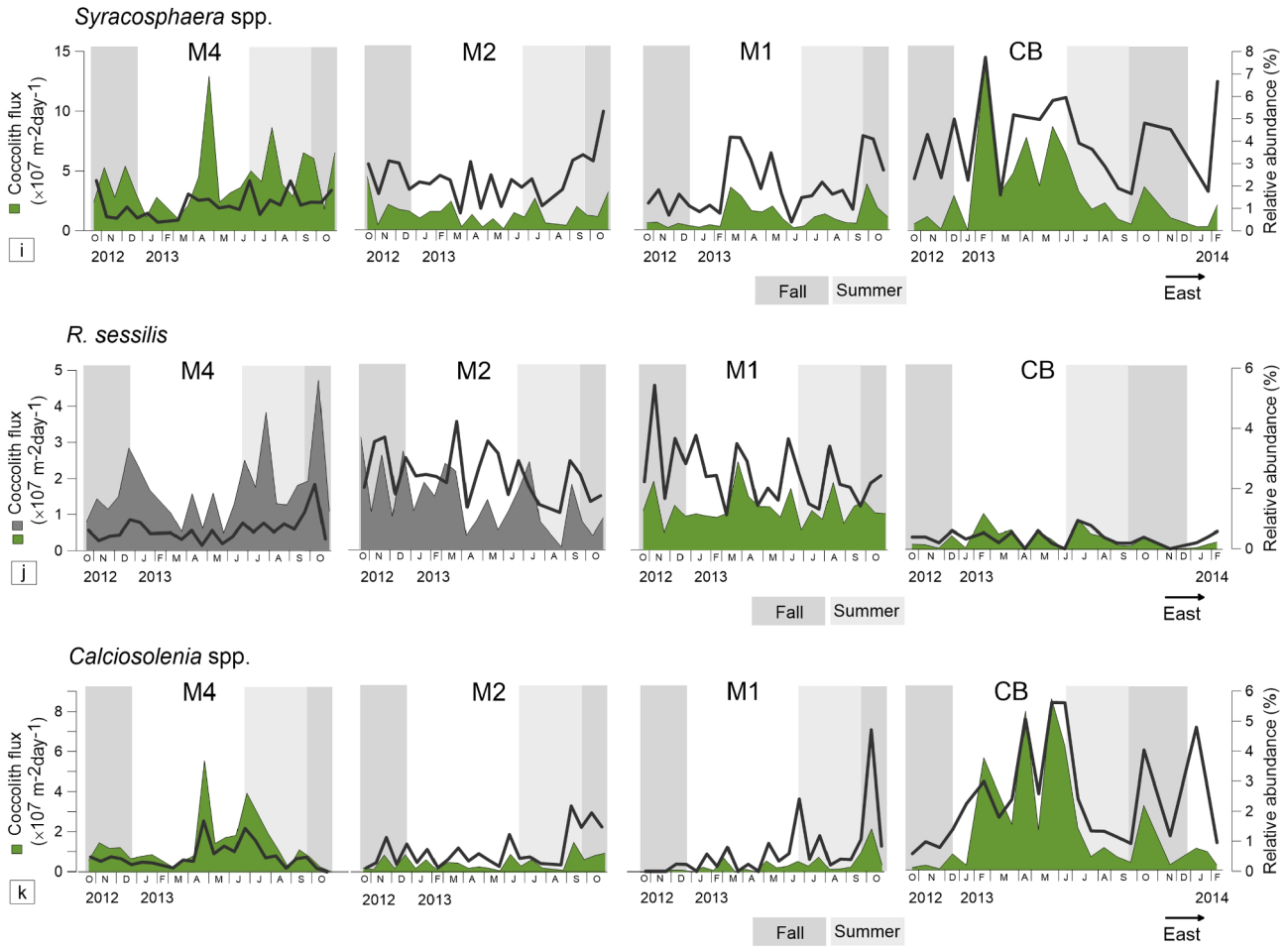

Fig. 6. (*continued*)

Highest coccolith fluxes of *C. leptoporus* at site CB agree with its higher abundance in the UPZ (Haidar and Thierstein, 2001) in upwelling-influenced regions, and towards the eastern equatorial Atlantic (Kinkel et al., 2000; Boeckel et al., 2006; Baumann et al., 2016). Although *Umbilicosphaera* species are usually found associated with warm and oligotrophic environments (Winter et al., 1994, 2002; Young, 1994; Haidar and Thierstein, 2001; Baumann et al., 2016), some species (i.e. *U. sibogae*) have been included in the predominantly bloom-forming group of coccolithophores, together with other placolith-bearing taxa (Baumann et al., 1999). *Umbilicosphaera* spp. were also found to increase in sediments underneath more productive waters in the central-eastern equatorial Atlantic (in Boeckel et al., 2006), consistent with our transatlantic observations. Also *Syracosphaera* spp. were most abundant at site CB (Figs. 6i and 7c), suggesting a similar preference for nutrient rich shallower waters (e.g. Andruleit and Rogalla, 2002; Andruleit, 2007) although their wider transatlantic distribution also links them to oligotrophic conditions in transitional environments (Young, 1994; Andruleit and Rogalla, 2002) without a particular depth preference (Andruleit et al., 2003; Poulton et al., 2017). Such discrepancies may reflect the species diversity within *Syracosphaera*, with distinct ecologies (see Baumann et al., 2008) in different environmental niches (see Poulton et al., 2017) both vertically across the photic layer and horizontally across the tropical North Atlantic. For *Calciosolenia* spp. higher abundances at site CB suggest an affinity for nutrient enrichment near the surface, as it may also occur at higher latitudes in the subtropical gyres and temperate open Atlantic (Baumann et al., 2008; Narciso et al., 2016; Poulton et al., 2017) and in the equatorial upwelling region (Poulton et al., 2017).

Lower coccolith export fluxes at the sites M1 and M2 reflect the lower sea surface Chl-*a* concentrations and weakest seasonality in the more stable and thermally stratified southeastern and central part along the transect (Fig. 7a). Slightly higher fluxes of *F. profunda*, *G. flabellatus*, *Umbellosphaera* spp., *Rhabdosphaera* spp. and *R. sessilis* during summer and fall in these areas (Fig. 6a, e, j), more noticeable at M2, seem related to the highest SSTs and strongest stratified water conditions during these seasons (Fig. 7b). This appears to reflect the northward seasonal migration of the ITCZ during summer and fall (Basha et al., 2015; Guerreiro et al., 2017), as indicated by much higher precipitation rates and weaker winds along 12° N (Fig. 6a). Site M1 was marked by persistently higher abundances of *Helicosphaera* spp. (Figs. 6f and 7c), a group that is often regarded part of the UPZ flora thriving in the North Atlantic subtropical gyre (Haidar and Thierstein, 2001; Narciso et al., 2016; Poulton et al., 2017). However, their prominence at M1 as opposed to CB does not support a clear affinity for more mesotrophic conditions in a well-mixed upper water column (Haidar and Thierstein, 2001; Boeckel et al., 2006; Ziveri et al., 2004) as earlier reported from high percentages in sediments offshore upwelling-influenced coastal regions (off W Iberia, Guerreiro et al., 2015; NW Africa and Benguela Current Upwelling System, Boeckel et al., 2006). In fact, site M1 revealed slightly weaker winds and a shallower MLD compared to M2 and M4 (Fig. 7a and b), suggesting even more stable conditions. We propose that the higher UPZ/LPZ ratios at M1 than M2 are reflecting a more nutrient-enriched UPZ related to the eastward shoaling of the nutricline (see Fig. 2; see Section 5.2) and to its proximity to water masses influenced by offshore upwelling associated with the Guinea Dome (Siedler et al., 1992).

Our new data show a clear westward gradient from CB of increasing LPZ species (*F. profunda* and *G. flabellatus*) and a more oligotrophic-UPZ

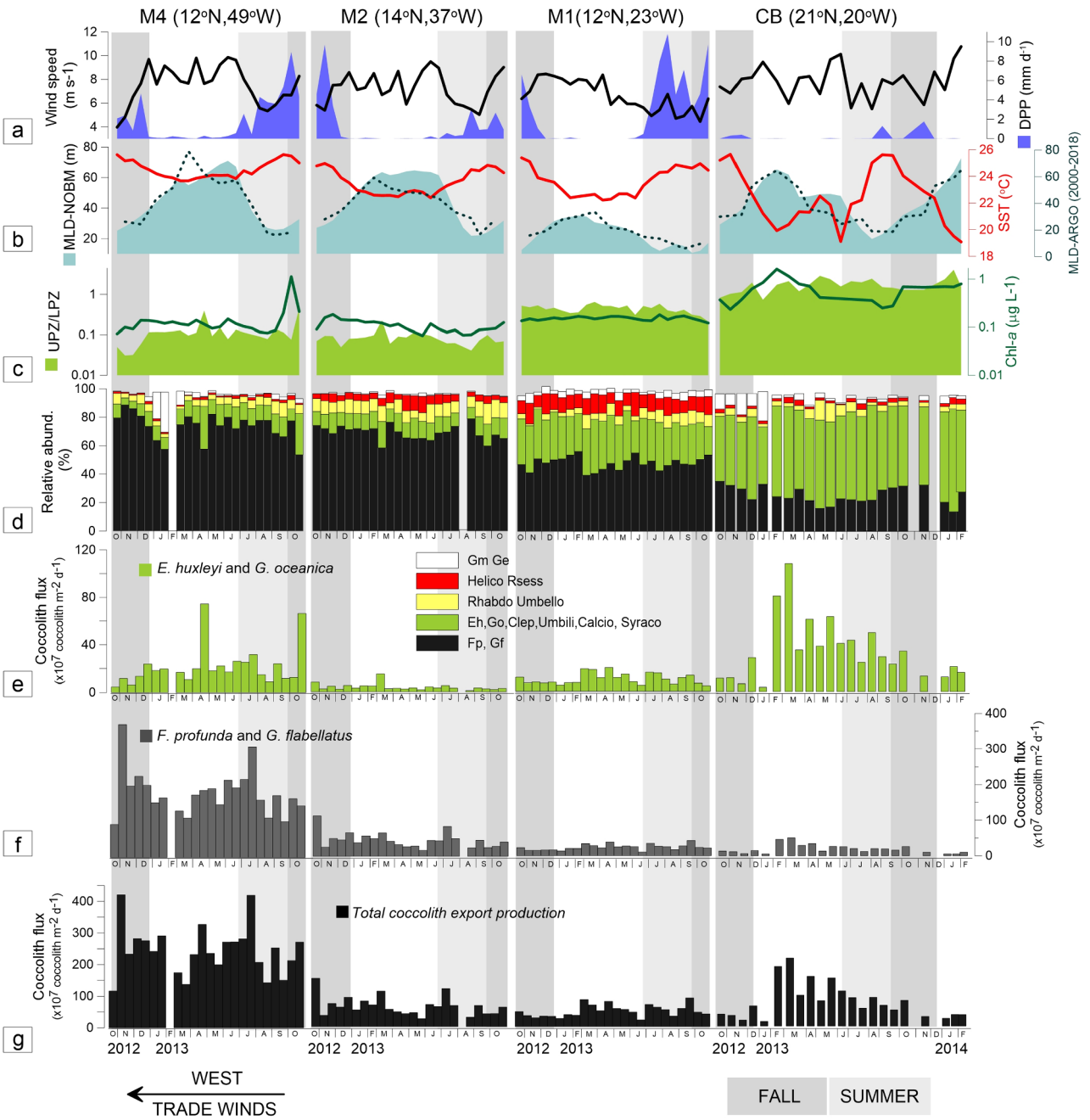

Fig. 7. Spatiotemporal variation of (a) daily precipitation rates (blue) and wind speed (black line), (b) seasonal mixed layer (MLD) from the NASA Ocean Biogeochemical Model (NOBM) (light blue, 2012–2013), MLD monthly climatology obtained from the in situ data measured by Argo floats (dashed curve, 2000–2018), and sea surface temperature (SST), (c) UPZ/LPZ ratios (light green), sea surface Chl-*a* concentrations (dark green line) and SST (red line), (c) relative abundance of the most abundant taxa (> 3%), (d) coccolith fluxes by the UPZ species *E. huxleyi* and *G. oceanica* (green), (e) coccolith fluxes by the LPZ species *F. profunda* and *G. flabellatus* (grey) and (f) total coccolith export fluxes (black) at sites M4, M2, M1 and CB. Taxa with a similar spatiotemporal distribution were grouped (Gm = *G. muellerae*; Ge = *G. ericsonii*; Helico = *Helicosphaera* spp.; Rsess = *R. sessilis*; Rhabdo = *Rhabdosphaera* spp.; Umbello = *Umbellosphaera* spp.; Eh = *E. huxleyi*; Go = *G. oceanica*; Clep = *C. leptoporus*; Umbili = *Umbilicosphaera* spp.; Calcio = *Calciosolenia* spp.; Syraco = *Syracosphaera* spp.; Fp = *F. profunda*; Gf = *G. flabellatus*). Most data for M2 and M4 presented in this figure are from Guerreiro et al. (2017), with the exception of the percentages of *G. ericsonii*, *C. lepotporus*, *Syracosphaera* spp. and *Calciosolenia* spp. UPZ/LPZ calculated from the ratio between the UPZ-species *E. huxleyi* and *G. oceanica*, and LPZ-species *F. profunda* and *G. flabellatus* (see Section 2.2) and MLD data. (For interpretation of the references to colour in this figure legend, the reader is referred to the web version of this article.)

assemblage (e.g. *Umbellosphaera* spp., *Rhabdosphaera* spp.) towards the central-western tropical North Atlantic (see Guerreiro et al., 2017). Persistently low abundances of *E. huxleyi* and gephyrocapsids (Figs. 6b–d and 7d) and the lowest and narrowest range of UPZ/LPZ ratios at site M2 (Fig. 7b) testify to a more oligotrophic environment. This is corroborated by highest percentages of *F. profunda*, *Umbellosphaera* spp. and *Rhabdosphaera* spp. (Figs. 6a, e and 7c), all of which known for their high affinity for warm and highly-stratified conditions typical of tropical and subtropical open-ocean regions (Haidar and Thierstein, 2001; Kinkel et al., 2000; Winter et al., 2002; Poulton et al., 2017). Also belonging to this group is the poorly known *R. sessilis*, given the enhanced percentages at the most oligotrophic site (M2) in the central part of the transect (Figs. 6j and 7c), often found associated with the LPZ and forming symbiotic colonies around diatoms (Hagino et al.,

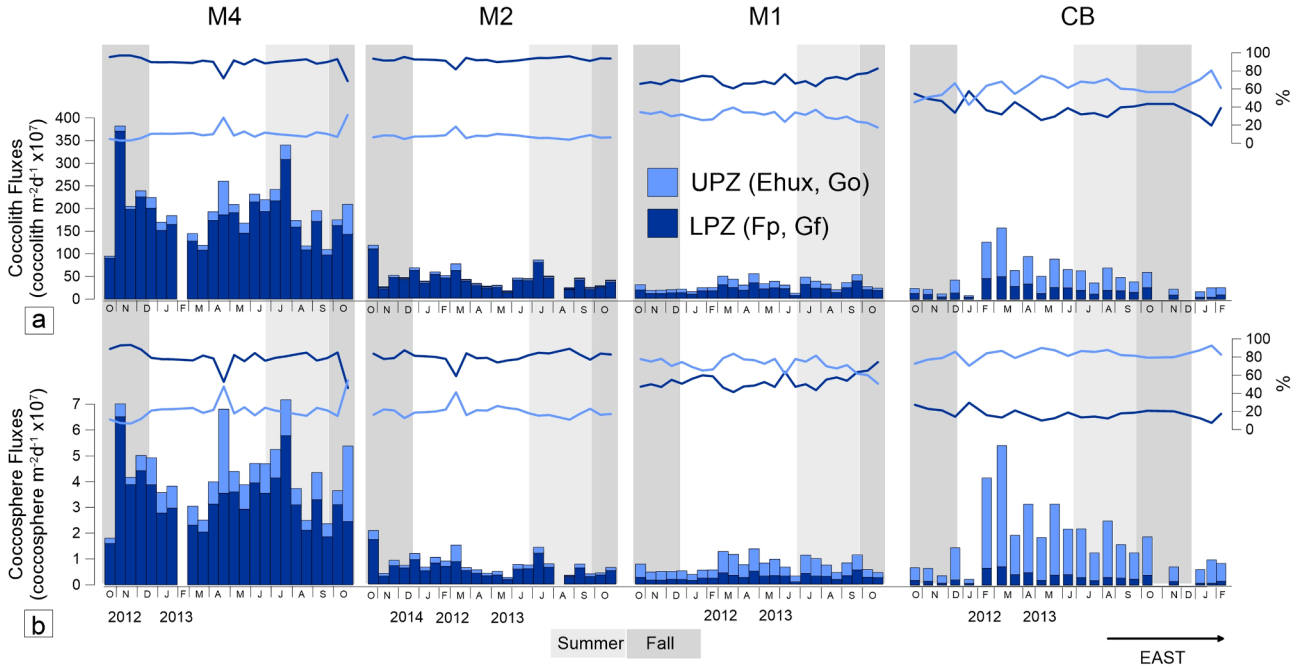

Fig. 8. Spatiotemporal variation in (a) total coccolith export fluxes (coccolith $m^{-2} d^{-1}$) and (b) total coccosphere export fluxes (coccosphere $m^{-2} d^{-1}$) of UPZ species (*E. huxleyi* and *G. oceanica* – light-blue bars) and LPZ species (*F. profunda* and *G. flabellatus* – dark-blue bars), at trap sites M4, M2, M1 and CB. Relative abundances of UPZ species and LPZ species are indicated in light-blue and dark-blue lines, respectively. Conversion of coccolith fluxes into coccosphere fluxes based on measurements performed by Knappertsbusch (1993) (i.e. 23 liths per sphere for *E. huxleyi* and 76 liths per sphere for *F. profunda*), Winter and Siesser (1994) (i.e. 40 liths per sphere for *G. flabellatus*), Yang and Wei (2003) (i.e. 70 liths per sphere for *F. profunda elongata*) and Kleijne et al. (2002) (i.e. 22 liths per sphere for *G. oceanica*). Coccolith fluxes from sites M2 and M4 were previously published (Guerreiro et al., 2017). (For interpretation of the references to colour in this figure legend, the reader is referred to the web version of this article.)

2017; Poulton et al., 2017).

Site M4 stands out as a region of exceptionally high coccolith fluxes considering its tropical open-ocean environmental background (Guerreiro et al., 2017), as revealed by its 3–5 times higher coccolith fluxes compared to even the upwelling-influenced site CB (Figs. 4 and 7g). Occasional aggregates and/or faecal pellets containing organic material and coccoliths in samples collected at CB, compared to the organic-free material that was analysed for M1, M2 and M4 (see Section 3.2), might have resulted in slightly under-evaluated coccolith fluxes offshore Cape Blanc. Likewise, higher lith/sphere ratios of the LPZ species (e.g. ~30–100 liths per sphere of *F. profunda*; Okada and Honjo, 1973) compared to, e.g. *E. huxleyi* (~9–50 liths per sphere; Cros and Fortuño, 2002) will also have overestimate coccolithophorid rather than coccolith export productivity of LPZ species at site M4 (see Guerreiro et al., 2017). Indeed, when comparing the coccosphere fluxes (converted from total coccolith fluxes; see Yang and Wei, 2003, and authors therein) from the UPZ species (*E. huxleyi* and *G. oceanica*) and from the LPZ species (*F. profunda* and *G. flabellatus*), the first do increase in relation to the latter, hence weakening the contrast between both ends of the transatlantic transect (Fig. 8). However, site M4 still remains the most productive of the four sites, reinforcing our hypothesis of particularly favourable conditions for the development of the LPZ flora. The westward deepening of the nutricline and the occurrence of diapycnal mixing between the nutrient-rich Antarctic Intermediate Water and the overlying water masses (Pelegrí et al., 2017) could have contributed to the very high fluxes of the LPZ flora in this area.

5.1.2. Comparison with other flux studies in the North Atlantic

Whereas the dominance of *E. huxleyi* at site CB is consistent with previous trap studies in this region (Köbrich and Baumann, 2009) and in the CVB (Bory et al., 2001), we find lower mean coccolith fluxes, also compared to other locations further north (e.g. NABE-34, Broerse et al, 2000). Much higher fluxes previously reported for the CVB (417×10^7 coccoliths $m^{-2} d^{-1}$ at ~18°N; Bory et al., 2001) and for CB (182×10^7 coccoliths $m^{-2} d^{-1}$ ~21°N; Köbrich and Baumann, 2009), may be driven by enhanced interannual variability in this region. This hypothesis is supported by previous studies reporting particle fluxes off Cape Blanc that have a much more pronounced interannual variability compared to a very low seasonality (Ratmeyer et al., 1999; Bory et al., 2001; Lathuilière et al., 2008; Fischer et al., 2009b; Fischer et al., 2016). The "giant filament" in this region, however, has been reported to show strong spatiotemporal variability depending on the intensity of the wind stress (Morel, 1996; Morel, 2000). Weaker wind-forcing could have contributed to lower coccolith fluxes and increase the mean percentage of *F. profunda* (12–34%, Table 2) during 2012–2014 at site CB compared to 1988 –1989 in the same region (6–19%; Köbrich and Baumann, 2009) (Fig. 9b). It could also reflect a weakening of coastal upwelling offshore Cape Blanc in recent times, as discussed in Section 5.3. Much higher fluxes south of the CVFS (Bory et al., 2001) may also reflect the higher proximity of this trap location to the influence of yearlong offshore upwelling at the Guinea Dome (see Pelegrí et al., 2017).

Regarding trap M4, this region clearly stands out for showing very high mean coccolith fluxes also in relation to previous trap records from other regions in the North Atlantic (Fig. 9a), including open-ocean temperate and subtropical settings (e.g. Broerse et al., 2000; Sprengel et al., 2002), the vicinity of islands (Sprengel et al., 2002), and areas of coastal upwelling (Beaufort and Heussner, 1999; Köbrich and Baumann, 2009). The only exception regards trap station "M" in the Cape Verde Basin (CVB), where Bory et al. (2001) reported bulk coccolith fluxes 5 times higher compared to M4. Whereas the UPZ fast-blooming *E. huxleyi* was the dominant species in all these previous trap studies, site M4 was dominated by the LPZ species *F. profunda* and *G. flabellatus*. We also note a general northward increase of the ratio between the percentages of *E. huxleyi* and *F. profunda* (i.e. Eh/Fp; Fig. 9b), with the lowest ratios recorded along our tropical transatlantic transect (~12°N) and the highest ratios at the subtropical site NABE-34 (Broerse et al., 2000) and at the temperate upwelling-influenced site ECOFER-

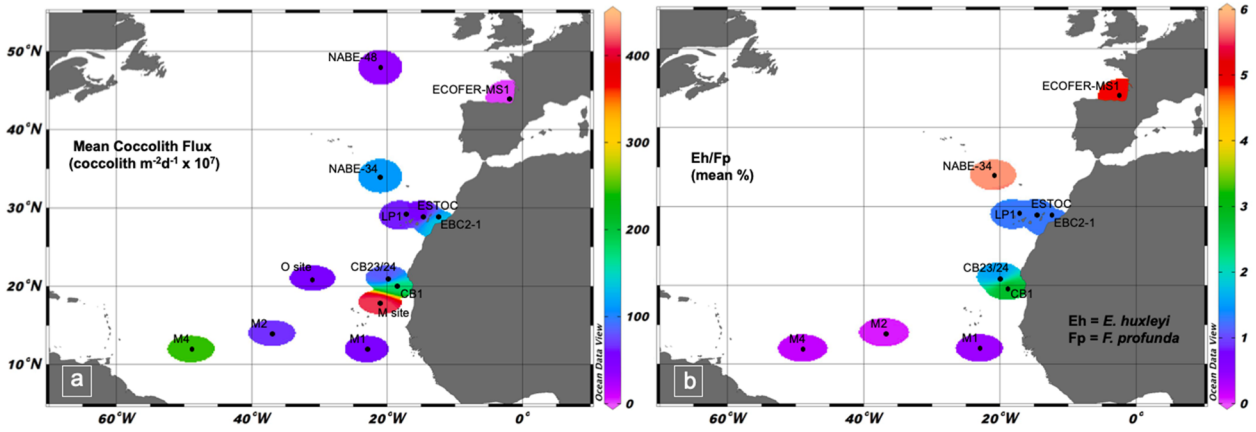

Fig. 9. Comparison between the (a) mean coccolith fluxes (coccolith $m^{-1}d^{-1}$) and (b) ratio between the mean percentages of *E. huxleyi* and of *F. profunda* presented in this study and from other sediment trap studies undertaken in the North Atlantic: NABE-48 and NABE-34 (April 1989 to April 1990) from Broerse et al. (2000), LP1, ESTOC and EBC2-1 (January to September 1997) from Sprengel et al. (2002), ECOFER-MS1 (June 1990 to August 1991) from Beaufort and Heussner (1999), CB1 (March 1988 to March 1989) from Köbrich and Baumann (2009), O site and M site (February 1991 and November 1992) from Bory et al. (2001), M2 and M4 from Guerreiro et al. (2017) and CB and M1 from this study. For NABE-48, O site and M site, there are no data available for both species, whereas for LP1, ESTOC and EBC2-1 Sprengel et al. (2002) only provide mean percentages for all three sites.

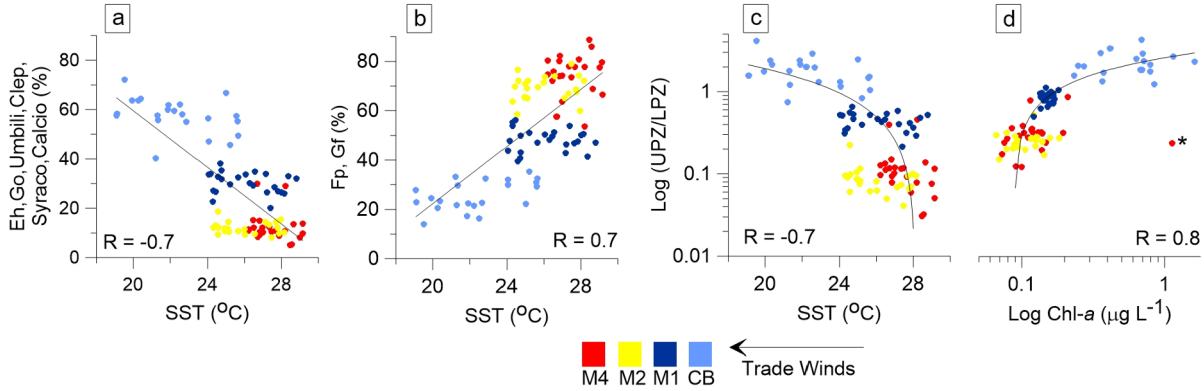

Fig. 10. Basin-scale correlations between SST and relative abundances of the coccolithophore taxa (mean > 3%) that increased in upwind direction (a) and in downwind direction (b), between the log ratio of UPZ/LPZ and SST (c) and Chl-*a* concentrations (d) at mooring stations M4, M2, M1 and CB (Eh – *E. huxleyi*, Go – *G. oceanica*, Clep – *C. leptoporus*, Umbil – *Umbilicosphaera* spp., Syraco – *Syracosphaera* spp., Calcio – *Calciosolenia* spp., Fp – *F. profunda*, Gf – *G. flabellatus*). In (d) sample outlier M4-24 (indicated in red, with an asterisk) was not included in the regression regressions. (For interpretation of the references to colour in this figure legend, the reader is referred to the web version of this article.)

MS1 (Beaufort and Heussner, 1999). This agrees well with the increased thermal stratification towards the tropics, hence benefiting the development of the LPZ flora. Nevertheless, mean bulk coccolith fluxes at M2 and M1 are similar in magnitude to fluxes reported further north, at higher latitudes in the North Atlantic (NABE-48, Broerse et al., 2000; LP1 and ESTOC, Sprengel et al., 2002; station O, Bory et al., 2001) (Fig. 9a). This suggests that coccolith export production in the tropics may be higher than originally expected, in spite of the absence of a winter mixed layer that is deep enough to break the deep pycnocline (Fig. 3 and 6b) at these latitudes (Levitus, 1982).

5.2. Transatlantic wind-forced ecological gradients

As the NE trade winds continuously force the surface waters to flow westwards across the North Atlantic equatorial region, the thermocline and the nutricline become significantly deeper further west (Merle, 1980a,b; Katz, 1981; Figs. 2 and 3). Such deepening is forced by a combination of the NE trade winds with the Coriolis effect (Merle, 1980a,b; Katz, 1981) and appears to be a permanent feature in this area, not only throughout the year (Fig. 3) but also in the annual mean climatology for 1955–2017 (Fig. 2). By contrast, the MLD does not show a clear W-E gradient but a seasonal dynamics that is similar to that of wind speed (Figs. 3 and 7a, b). This suggests that the trade winds forcing over the uppermost ~75–80 m had a similar magnitude along most of the transect (see Fig. 7a). However, due to the westward geostrophic deepening of the thermocline/nutricline (see Figs. 2 and 3), the effects of such mixing are notably distinct in terms of the thermocline/nutricline dynamics at both ends of the transect. Since towards west, the thermocline/nutricline is persistently below the MLD throughout the year (Figs. 3 and 7b), such mixing is not deep enough to promote nutrient-enrichment of the upper photic zone (see Figs. 2 and 3). Concurrently, as the thermocline/nutricline becomes increasingly shallower towards the east (Fig. 3), it becomes ence increasingly positioned within the wind-forced mixed layer, hence leading to nutrient-enrichment of the upper water column. This is clearly shown in the much more marked seasonal variation of SST at site CB (Fig. 7b).

These basin-scale wind-forced gradients are strikingly reflected in the transatlantic variations of the coccolith fluxes we observed for 2012–2013 (Figs. 6 and 7). Increasing abundances of the LPZ species *F. profunda* and *G. flabellatus* from NW Africa to the Caribbean (Fig. 7e), accompanied by decreasing UPZ/LPZ ratios and surface Chl-*a* concentrations at increasing SST (Fig. 7b), are related to the geostrophic deepening of the thermocline/nutricline towards west. These trends are also reflected in positive correlations between the LPZ flora and SST, and negative correlations between these species and surface water Chl-*a* concentrations (Fig. 10). Concurrently, decreasing abundances of the

UPZ r-selected species *E. huxleyi* and *G. oceanica* towards west (Fig. 7b and d), accompanied by an increase in SST and a decrease in both surface Chl-*a* concentrations and UPZ/LPZ ratios (Fig. 7b), are related to the eastward shoaling of the nutricline/thermocline and associated increase of surface productivity. Although less strikingly than *E. huxleyi* and *G. oceanica*, other taxa also decrease westward, i.e. *C. leptoporus*, *Umbilicosphaera* spp. and *Calciosolenia* spp. (Fig. 7c). These gradients are strongest between sites CB and M2, with highly negative correlations between the UPZ flora and SST, and positive correlations between UPZ species and Chl-*a* concentrations (Fig. 10). The same E-W gradient remains after converting coccolith fluxes into coccosphere fluxes, in spite of a slight increase of the UPZ species at all four sites (see Fig. 8). Previous studies based on snapshot observations of living coccolithophore communities and on time-averaged coccolith assemblages from core top sediments had already related similar E-W ecological changes with basin-scale deepening of the nutricline along the equatorial and South Atlantic (Kinkel et al., 2000; Boeckel et al., 2006; Baumann et al., 2008). Our seasonally resolved 1-year of transatlantic fluxes fully corroborates these studies by providing particularly robust evidence of such geostrophic wind-forced ecological gradients, highlighting the validity of using the UPZ/LPZ ratio as a proxy for inferring variations in the depth of the nutricline when dealing with paleoreconstructions (e.g. Molfino and McIntyre, 1990; Guerreiro et al., 2017).

Westward deepening of the nutricline was also reflected in seasonal differences between species with opposing ecological preferences along the transatlantic transect: highest abundances of *F. profunda* and *G. flabellatus* during the fall 2012 and the summer 2013 (Fig. 7e), versus highest abundances of *E. huxleyi* and *G. oceanica* during the spring and fall 2013 at site M4 (Fig. 7d). This contrasts with the sites eastwards of M4, where most coccolithophore species revealed increasingly similar seasonal patterns in concert with the gradual shoaling of the thermocline/nutricline. This suggests that the entire photic zone becomes increasingly prone to nutrient-enrichment towards the east whenever wind-forced turbulence and mixing occurs, hence favouring both UPZ- and LPZ-species. In contrast, an increasingly deeper nutricline further west will promote the proliferation of seasonally distinct species at different water depths by increasing the vertical partitioning of ecological niches within the photic zone (in O'Brien et al., 2016).

The observed oceanographic gradients also appeared to affect species diversity. Whereas the total number of species identified was rather similar amongst the four mooring sites, we found significant differences in terms of Shannon–Weaver diversity index (H′) between the north-eastern and western-central parts of the transect. Persistently higher H′ values at the eastern and upwelling-influenced sites CB and M1 (Figs. 4 and 5) suggest that higher nutrient availability not only promoted the increase of r-selected surface-dwelling species, but also a more even distribution of species relative abundances. This appears to contradict earlier plankton studies reporting lower species richness and higher species dominance in nutrient-enriched temperate and coastal upwelling regions compared to the nutrient-depleted subtropical gyres and equatorial waters (Ottens and Nederbragt, 1992; Winter et al., 1994; Cermeño et al., 2008; Poulton et al., 2017; Charalampopoulou et al., 2011). Much higher Saharan dust deposition closer to NW Africa (Ratmeyer et al., 1999; Romero et al., 2003; Korte et al., 2017; van der Jagt et al., 2018) could have promoted a faster, and hence, more protected sinking of coccospheres from the photic layer down to the deep sea, increasing the chances of preserving the original species diversity at sites CB and M1 (e.g. Köbrich et al., 2015). On the other hand, if such was the case, one would expect that the same processes would be also reflected in higher total coccolith fluxes in the east compared to further west since total mass fluxes were much higher close to Africa (Figs. 4 and 5). However, this was not the case during the monitored period. Furthermore, positive correlations between total mass flux and total coccolith flux at all four sites suggest they contributed similarly along the entire transect, and quite independently from the dust source in Africa (Fig. 5a-d). Weak correlations between H′ and total mass fluxes, combined with opposite correlation trends between CB and M1 (Fig. 5e–h) strongly suggest that H′ is mostly reflecting the original differences in species diversity rather than differences in magnitude of biostratinomic processes (Müller, 1963) along the transect.

Holococcolith species were rare and mostly belonging to the genus Syracolithus found at sites M2 and M4 (e.g., *S. dalmaticus*, *S. schilleri, S. ponticuliferus*; see taxonomic appendix in the Supplementary Material) and contributed little to H′-diversity. As K-selected species, their contribution may have been larger in the oligotrophic UPZ conditions found in these sites (e.g. Kleijne, 1991; Houdan et al., 2006; Dimiza et al., 2008; Cros and Estrada, 2013), which could reflect their reportedly higher susceptibility to dissolution (Kleijne, 1991; Cros, 2001). However, this conflicts with recent findings by Triantaphyllou et al. (2018), reporting unexpectedly high resistance of holococcolithophores to decreased pH conditions in the NE Mediterranean. Some studies have also reported an affinity of holococcolithophores for shallower coastal conditions (Triantaphyllou et al., 2002) and higher abundances of these species in the eastern North Atlantic (Kleijne, 1991). Köbrich et al. (2015) however, reported to enhanced fluxes abundance and species diversity of holococcoliths during a fast and very high particle flux event at site CB, supporting a broader ecology for these species and suggesting a greater propensity to be laterally advected rather than dissolved. If present at all in our study area, holococcolithophores are more likely to have been laterally advected (see Köbrich et al., 2015), subjected to mechanical breakage by zooplankton grazers (Knappertsbusch and Brummer, 1995) or simply fallen apart in during the processing of the sediment trap samples. These processes would have reduced holococcoliths to individual calcite rhombs of submicron size that probably disappeared through the 0.4 μm filter pores. To more accurately assess the extent to which post-mortem processes affected holococcolithophores such that it may have contributed to lower the H′s at M4 and M2, compared to M1 and CB, more information would be required on the coccolithophore communities living in the study area.

5.3. Coccolithophores in a warming ocean

Zooming out the transatlantic transect to a broader region in the tropical Atlantic, our sampling period revealed a SST spatial pattern (Fig. 11b) that is similar to the annual SST means calculated from MODIS-Aqua satellite data (2003–2017) (Fig. 11a), as well as from WOA which is based on in situ observations (1955–2017; Fig. 11d). Site CB, influenced by coastal upwelling of NW Africa, clearly figures as the persistently coolest of the four studied locations, as opposed to M4 which figures as the persistently warmest. Interestingly however, the SST anomalies for the sediment-trap period clearly show a warm anomaly across the entire transect compared to the annual mean from 2003 to 2017 (Fig. 11c). This is particularly noticeable at the eastern-most sites CB and M1 (Fig. 11c), suggesting increased thermal stratification and, subsequently, a weaker influence of coastal and offshore upwelling in the two regions during the sampling period. This is consistent with the observed higher percentages of *F. profunda* and lower percentages of *E. huxleyi* offshore Cape Blanc (i.e. 12–34% and 14–51%, respectively) for 2012–2014, compared to 1988 –1989 (6–19% and 30–45% for *F. profunda* and *E. huxleyi*, respectively; Köbrich and Baumann, 2009) (see Fig. 8).

Our observations are supported by several studies reporting on unequivocal decrease of global phytoplankton concentration over the past century due to the increasing ocean warming and water column stratification, resulting in decreasing nutrient availability and marine production (e.g. Behrenfeld et al., 2006; Polovina et al., 2008; Belkin, 2009; Boyce et al., 2010; Signorini and McClain, 2012; Bopp et al., 2013; Hoegh-Guldberg et al., 2014; Krumhardt et al., 2017). According to the last IPCC report, the Atlantic Ocean has warmed more than any other ocean basin (0.3 °C per decade) since the 1970s (Hoegh-Guldberg et al., 2014). This has resulted in the advancing of relatively warm Atlantic waters northwards and eastwards (Årthun et al., 2012), and

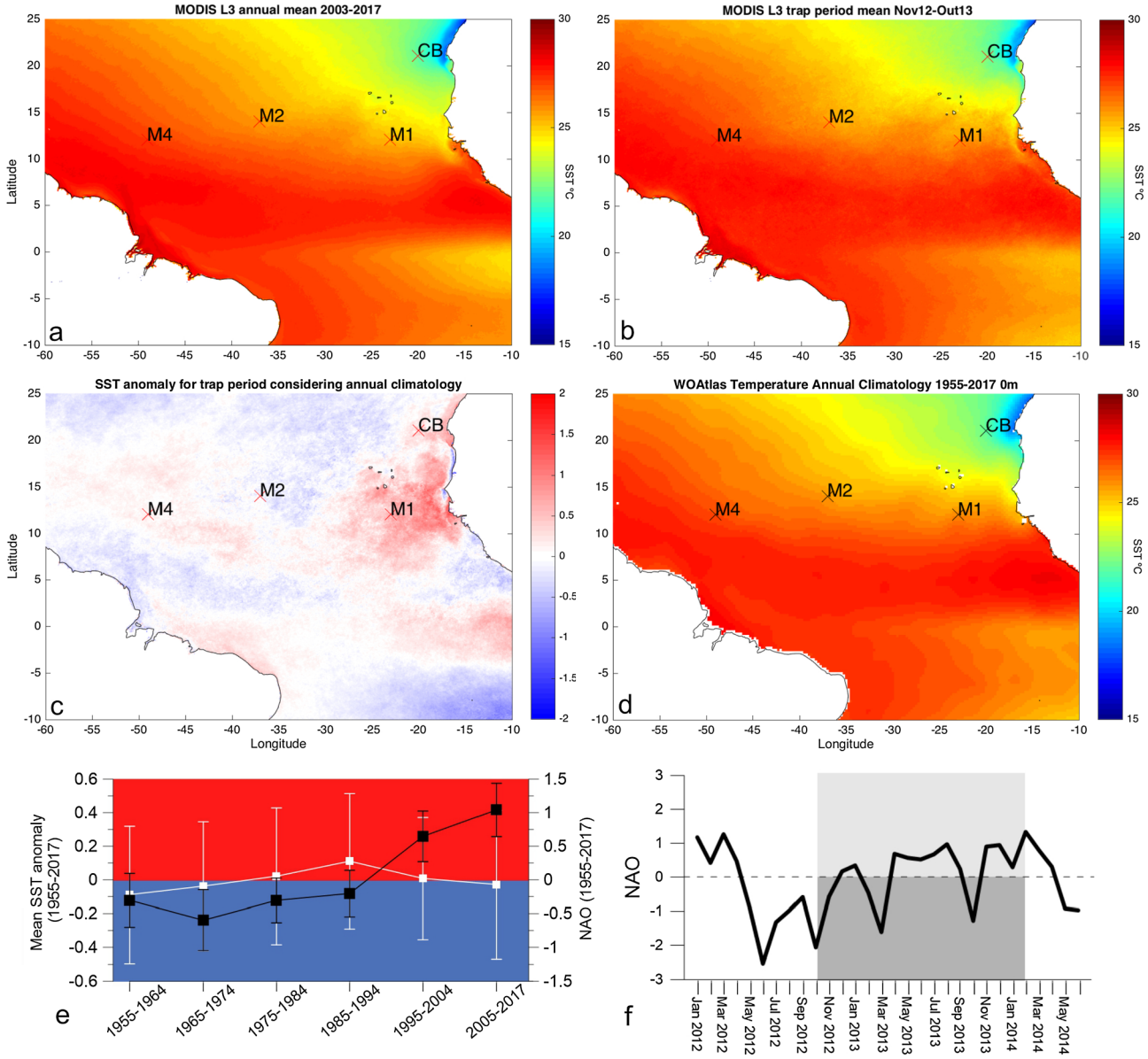

Fig. 11. (a) Sea surface temperature (SST) annual climatology computed using 15 yearly-composites of MODIS-Aqua SST 11 μm night product 4 km-resolution; (b) SST mean for the trap-sampling period, MODIS-Aqua L3 data 4 km resolution; c) trap-sampling period SST anomaly map for the region calculated as (b)–(a); d) World Ocean Atlas (WOA) SST annual climatology (1955–2017), (e) respective decadal mean SST anomalies for the study area and decadal mean variation of the North Atlantic Oscillation (NAO), and (f) NAO variation for the sediment-trap monitored period.

about 4% increase of thermal stratification between the surface and 200 m from 1971 to 2010 in all parts of the ocean north of 40°S (Hoegh-Guldberg et al., 2014 and refs. therein). Estimates based on model simulations indicate a climatically-driven decrease in phytoplankton productivity in the oceans by 50% during the current century (Falkowski and Oliver 2007) and a drop of 8.5% between 1960 and 2006 (Laufkoetter et al., 2013). Moore et al. (2018) have recently predicted a decrease by nearly 60%, 24% and 41% of the potential fishery stocks, primary production and carbon export, respectively, due to warming-driven decreased vertical mixing and exchange between the upper and the deep ocean, with the highest nutrient declines occurring in the North Atlantic. Other models, included in the Coupled Model Intercomparison Project Phase 5 (CMIP5) also show an overall warming-driven decrease in global net primary production over the mid-21st century, particularly in tropical and subtropical regions, and in most of the Atlantic Ocean (Krumhardt et al., 2017)

The decline in the tropical and subtropical net primary productivity since 1999 due to the increase of water thermal stratification (e.g. Behrenfeld et al., 2006) appears to have been followed by a large reduction in the diversity of tropical phytoplankton (Thomas et al., 2012) and an increase and northward expansion of small-celled phytoplankton such as coccolithophores and N-fixing cyanobacteria (Rivero-Calle et al., 2015; Krumhardt et al., 2016, 2017). Such northwards expansion is thought to reflect their higher advantage at competing for nutrients in strongly-stratified oligotrophic conditions compared, for instance, to diatoms (Katz et al., 2004; Morán et al., 2010; Boyd et al., 2010; Lancelot et al., 2012; Krumhardt et al., 2017).

Polovina et al. (2008) proposed a mechanism of gyre expansion, through which the most oligotrophic and least productive regions of the gyres start to expand as they become warmer and more stratified, particularly in the North Atlantic. Whereas the increasing land-ocean thermal contrast due to gyre expansion is thought to intensify upwelling-favouring winds off NW Africa (the so called “Bakun Upwelling Intensification Hypothesis”, Bakun, 1990; McGregor et al., 2007;

Cropper et al., 2014), other studies describe wind trends in the Canary Upwelling system as being equivocal and even weakening (e.g. Sydeman et al., 2014; García-Reyes et al., 2015). According to the last IPCC report, the Eastern Boundary Upwelling Ecosystem (EBUE) associated to the Canary Current (CC) exhibited a significant rate of change in the average SST (0.12 °C per decade), and a significant temperature increase of the warmest month (0.11 °C per decade) between 1971 and 2010. Most observations suggest that the CC has warmed since the early 1980s, indicating a warming of 0.53 °C from 1950 to 2009 (Arístegui et al., 2009; Barton et al., 2013). Gómez-Gesteira et al. (2008) further suggested a 20 and 45% decrease in the strength of upwelling in winter and summer, respectively, from 1967 to 2006, consistent with a decrease in wind strength and direction over the past 60 years, and a decrease of primary production in the CC over the past 2 decades (Arístegui et al., 2009; Demarcq, 2009; Barton et al., 2013). Barton et al. (2013) projected that the distribution of most phytoplankton (including coccolithophores) will deepen and be less subjected to vertical mixing as the ocean warms off NW Africa. This is supported to some extent by the temporal variation of the averaged SST anomaly for our entire study area (Fig. 11e), which shows a gradual sea surface warming from 1955 to 2017 in the eastern tropical Atlantic, supporting a scenario of wind strength weakening. Our observations are consistent with Fischer et al. (2016), who also report no long-term trend of any particle flux component from 1988 to 2012 at site CB that would indicate intensified Mauritanian upwelling off Cape Blanc.

The North Atlantic Oscillation (NAO), which is the dominant mode of atmospheric variability in the North Atlantic Sector (Visbeck et al., 2003), has been referred to as a potential driver for attenuating or accentuating the overall warming trend, depending on the region (Hoegh-Guldberg et al., 2014 and refs. therein). The impact of the NAO index on primary production is assumed to be mediated through changes in meteorological forcing, such as enhanced wind-forced vertical mixing promoting nutrient enrichment in highly stratified tropical and subtropical open-ocean regions (Drinkwater et al., 2003). Positive index of the NAO has been associated to stronger trade winds and SST cooling from north Africa westward to the Caribbean, particularly during boreal winter (e.g. Hurrel et al., 2003; George and Saunders, 2001 and refs. therein). In situ increased levels of nutrients, chlorophyll and primary production observed at fixed stations in the subtropical North Atlantic (Hawaii Ocean Time-series – HOT; and Bermuda Atlantic Time-series Study - BATS) that contradict the general notion of ongoing unprecedented ocean warming rates, have been partially explained by such effects from a positive NAO index (see Hoegh-Guldberg et al., 2014 and refs. therein). Fisher et al. (2016) have also described a positive long-term trend between an increasing NAO index and fluxes of biogenic silica (proxy for diatom production) off Mauritania. One would expect to find such cooling during our monitored year since the latter was marked by a positive NAO index during most of the months (exceptions in November 2012, February-March 2013 and October 2013) (Fig. 11f). Yet, as referred above, the SST anomalies for 2012–2013 (Fig. 11c) illustrate the exact opposite, i.e. increasing SST along our transatlantic region. In addition, Fig. 11e also shows a tendency for the mean decadal NAO index to decrease since the mid 1980 s until the present, negatively correlated to the mean decadal variation of SST. If one considers that increasing SST is linked to upper ocean stratification, the decadal trend shown in Fig. 11e is in good agreement with the negative correlation between the NAO index and Chl-a earlier referred by Boyce et al. (2010) for the North- and Equatorial Atlantic (between 1899 and 2010). Piontkovski et al. (2006) also reports a negative correlation between the NAO index and total zooplankton biomass in the tropical and subtropical Atlantic regions from 1961 to 2001.

All these findings point to an increasingly warmer, stratified and oligotrophic upper ocean along the tropical North Atlantic having a negative impact on future coccolithophore species diversity. Whereas the UPZ species will likely be the most affected, species thriving in the LPZ might respond differently. Our observations suggest that the adaptation of *F. profunda* and *G. flabellatus* to the warm, stratified waters with a deep nutricline, reflects a potential competitive advantage in a future scenario of subtropical gyre expansion due to ocean warming. Mixotrophy and/or phagotrophy have been suggested as an alternative nutritional strategy for these species to thrive under the very low to nearly non-existent light levels in such tropical and subtropical open-ocean areas (Poulton et al., 2017), consistent with our transatlantic observations. Nevertheless, their seasonal co-occurrence with r-selected surface-dwellers where the nutricline is shallower (Figs. 2 and 3), suggests that they also respond positively to surface hydrological processes within a more seasonally dynamic ML. In other words, *F. profunda* and *G. flabellatus* may have more diverse nutritional strategies than other species, able to adapt more readily to changing environmental conditions. Although these species are not considered key taxa in terms of coccolith-carbonate production compared to large-sized (e.g. *C. leptoporus*) or fast-blooming placolith-bearing taxa (e.g. *E. huxleyi*) (Ziveri et al., 2007), their apparent competitive advantage may have implications for their future contribution to the biological pump and carbonate budget.

Results from our study emphasize the importance of understanding in more detail the ecological preferences of the LPZ flora, and of phytoplankton production across the entire photic zone when projecting the effects of ocean warming on future phytoplankton- and coccolithophore production. As most ecological and climate models dealing with global ocean productivity use surface Chl-*a* concentrations derived from remote-sensing observations, insights from the entire photic zone are likely to be a crucial addition. To confirm whether or not our sediment trap observations represent a unique “isolated” record or whether provide a modern analogue for the future ocean in the context of global climate warming, one would have to (1) calibrate our sediment trap and remote sensing observations with time-series of coccolithophore communities (cells per liter) living in this area and of hydrological parameters measured in situ (e.g. nutrients, CTD, irradiance, Chl-*a*); (2) extend our sediment trap time-series to evaluate potential interannual variability across the tropical North Atlantic; and (3) compare our study area with other W-E sections around the global tropical ocean.

6. Conclusions

Our synoptic observations of seasonally resolved export fluxes at four sediment trap sites contributes to understand the spatiotemporal variability of coccolithophore export production across the entire tropical North Atlantic. The main conclusions resulting from our study are as follows.

1. The westward increase of the LPZ species *F. profunda* and *G. flabellatus* and the concurrent decrease of the UPZ r-selected species *E. huxleyi* and *G. oceanica* follow the westward geostrophic deepening of the thermocline/nutricline across the tropical North Atlantic.
2. Up to 3–5 times higher coccolith fluxes at site M4 compared to the other sites, highlights the importance of the LPZ flora to the export coccolithophore fluxes in the open western tropical North Atlantic. Second highest coccolith export production at site CB, rich in UPZ and r-selected species is consistent with the production of filament-rich surface waters due to yearlong upwelling off Cape Blanc (NW Africa).
3. Lower coccolith export fluxes, weaker seasonality and the absence of intermittent maxima by more opportunistic taxa at sites M1 and M2 reflect comparatively more stable and less productive water conditions in the southeastern and central parts of the transect.
4. Seasonality was weak at all four sites. At M1, M2 and M4 latitudinal migration of the ITCZ led to warmer and more stratified conditions during summer and fall, which favoured the productivity of LPZ and UPZ-oligotrophic species, whereas cooler and less stratified conditions during winter and spring favoured the transient productivity of

r-selected and turbulence-resilient UPZ species (*E. huxleyi* and gephyrocapsids). Temporal changes in the intensity of wind-forced coastal upwelling at site CB caused higher UPZ/LPZ ratios and fluxes of most UPZ species, particularly in late winter.

5. The seasonal differences between more opportunistic species and LPZ and UPZ-oligotrophic taxa at westernmost site M4 suggest a higher vertical niche partitioning resulting from an increasingly deeper thermocline/nutricline further west. This contrasts with the similar seasonal patterns amongst species of contrasting light and nutrient requirements eastward of M4, reflecting the increasingly more uniformly nutrient-enriched mixed layer due to the eastward shoaling of the thermocline/nutricline.
6. Persistently lower diversity (H′) in the western and central tropical Atlantic appear to contradict the traditional view of oligotrophic regions as species-enriched compared to the more productive eastern boundaries and equatorial regions. Increased nutrient availability near the surface and a more dynamic upper ocean environment appeared to have promoted a more evenly distributed flora in terms of heterococccolithophore species relative abundances at eastern sites CB and M1.
7. *Florisphaera profunda* and *G. flabellatus* may have a competitive advantage in a future warmer ocean, with implications for their contribution to the biological pump and carbonate budget. We demonstrate the validity of the UPZ/LPZ ratio as proxy for the nutricline depth and emphasize the relevance of considering phytoplankton production across the entire photic zone when projecting the effects of ocean warming on future primary production and export of carbon to the deep ocean.

Acknowledgements

We thank the crews of Meteor cruise M89, Pelagia cruise 64PE378, RV Poseidon cruises P425, POS445 and POS464 (recovery of CB-24), as well as NIOZ and MARUM technicians for their contributions. Moorings M4, M2 and M1 managed by the Royal NIOZ in the framework of the multidisciplinary projects TRAFFIC funded by NWO (project no. 822.01.008), and DUSTTRAFFIC, funded by ERC (project no. 311152), both awarded to Jan-Berend W. Stuut. Moorings CB-23 and CB-24 managed by MARUM and the University of Bremen. We are deeply thankful to Gerhard Fischer for providing all the samples and total mass flux data from trap CB, and for his great and fruitful contribution during the discussion of the data and the writing of the manuscript. Lab preparation of the 1/5 split of the original sediment trap sample for M4, M2 and M1 was conducted at the NIOZ, whereas the splitting, filtering, and SEM taxonomical analysis were performed at the Geosciences Department of the University of Bremen, Germany. The first author benefited from a Marie Sklodowska-Curie Fellowship supported by the University of Bremen and the European Union FP7 COFUND under grant agreement no. 600411, and currently benefits from a Marie Sklodowska-Curie European Fellowship supported by the European Union H2020-MSCA-IF-2017 under grant agreement no. 796802. This study also had the support of the Portuguese Science Foundation (FCT), through the strategic project UID/MAR/04292/2013 granted to MARE, and the post-doctoral grant awarded to Carolina Sá (SFRH/BPD/118760/2016). Regarding the satellite data used in this study, the authors would like to acknowledge the following entities: the MODIS Atmosphere Science Team and the MODIS Adaptive Processing System (MODAPS); the NASA EOSDIS Physical Oceanography Distributed Active Archive Centre (PO.DAAC) (http://podaac.jpl.nasa.gov/SeaSurfaceSalinity/Aquarius); and the Ocean Biology Processing Group (OBPG) and the Atmosphere Archive and Distribution System (LAADS) at the NASA Goddard Space Flight Center. The CCMP version 2.0 vector wind analyses were produced by Remote Sensing Systems (www.remss.com) and the CMAP precipitation data were provided by NOAA/OAR/ESRL PSD, Boulder, Colorado, USA (http://www.esrl.noaa.gov/psd/). Modelled MLD data presented in Fig. 6 were obtained from the NASA Ocean Biogeochemical Model (https://gmao.gsfc.nasa.gov/reanalysis/MERRA-NOBM/), whereas the in situ MLD and temperature data presented in Figs. 3 and 6 were collected and made freely available by the International Argo Project, a pilot programme of the Global Ocean Observing System, and by the national programmes that contribute to it (http://www.argo.net). We are thankful to Afonso Ferreira for compiling the NAO time-series data downloaded from NOAA's Climate Prediction Center (https://www.cpc.ncep.noaa.gov/products/precip/CWlink/pna/nao.shtml). We also gratefully acknowledge the constructive criticism from the editors Nate Mantua and Josep Pelegri, and from two anonymous reviewers.

Appendix A. Supplementary material

Supplementary data to this article can be found online at https://doi.org/10.1016/j.pocean.2019.102140.

References

Alonso-González, I.J., Arístegui, J., Vilas, J.C., Hernandéz-Guerra, A., 2009. Lateral POC transport and consumption in surface and deep waters oft he Canary Current region: a box model study. Glob. Biogeochem. Cycles 23, GB2007.

Andruleit, H., 1996. A filtration technique for quantitative studies of coccoliths. Micropaleontology 42, 403–406.

Andruleit, H., 2007. Status of the Java upwelling area (Indian Ocean) during the oligotrophic northern hemisphere winter monsoon season as revealed by coccolithophores. Mar. Micropaleontol. 64, 36–51.

Andruleit, H., Rogalla, U., 2002. Coccolithophores in surface sediments of the Arabian Sea in relation to environmental gradients in surface waters. Mar. Geol. 186, 505–526.

Andruleit, H., Stager, S., Rogalla, U., Cepek, P., 2003. Living coccolithophores in the northern Arabian Sea: ecological tolerances and environmental control. Mar. Micropaleontol. 49, 157–181.

Arístegui, J., Barton, E.D., Álvarez-Salgado, X.A., Santos, A.M.P., Figueiras, F.G., Kifani, S., Hernández-León, S., Mason, E., Machú, E., Demarcq, H., 2009. Sub-regional ecosystem variability in the Canary Current upwelling. Prog. Oceanogr. 83 (1–4), 33–48.

Årthun, M., Eldevik, T., Smedsrud, L.H., Skagseth, Ø., Ingvaldsen, R.N., 2012. Quantifying the influence of Atlantic heat on Barents Sea ice variability and retreat. J. Clim. 25 (13), 4736–4743.

Bakun, A., 1990. Global climate change and intensification of coastal ocean upwelling. Science 247, 198–201. https://doi.org/10.1126/science.247.4939.198.

Barton, E.D., 1987. Meanders, eddies and intrusions in the Central Water Mass Front off NW Africa. Oceanol. Acta 10, 267–283.

Barton, E.D., Field, D.B., Roy, C., 2013. Canary Current upwelling: more or less? Prog. Oceanogr. 116, 167–178.

Basha, G., Kishore, P., Venkat Ratnamc, M., Ouarda, T.B.M.J., Velicogna, I., Sutterley, T., 2015. Vertical and latitudinal variation of the intertropical convergence zone derived using GPS radio occultation measurements. Remote Sens. Environ. 163, 262–269.

Baumann, K.-H., Cepek, M., Kinkel, H., 1999. Coccolithophores as indicators of ocean water masses, surface-water temperature, and paleoproductivity – Examples from the South Atlantic. In: Fischer, G., Wefer, G. (Eds.), Use of Proxies in Paleoceanography: Examples from the South Atlantic. Springer, Berlin, pp. 117–144.

Baumann, K.-H., Andruleit, H.A., Samtleben, C., 2000. Coccolithophores in the Nordic Seas: comparison of living communities with surface sediment assemblages. Deep-Sea Res. II 47, 1743–1772.

Baumann, K.-H., Boeckel, B., Cepek, M., 2008. Spatial distribution of living coccolithophores along an east-west transect in the subtropical South Atlantic. J. Nannoplankton Res. 30, 9–21.

Baumann, K.-H., Saavedra-Pellitero, M., Böckel, B., Ott, C., 2016. Morphometry, biogeography and ecology of Calcidiscus and Umbilicosphaera in the South Atlantic. Rev. Micropaléontol. https://doi.org/10.1016/j.revmic.2016.03.001.

Beaufort, L., Heussner, S., 1999. Coccolithophorids on the continental slope of the Bay of Biscay – production, transport and contribution to mass fluxes. Deep-Sea Res. Pt. II 46, 2147–2174.

Behrenfeld, M.J., O'Malley, R.T., Siegel, D.A., McClain, C.R., Sarmiento, J.L., et al., 2006. Climate-driven trends in contemporary ocean productivity. Nature 444, 752–755.

Boeckel, B., Baumann, K.-H., 2008. Vertical and lateral variations in coccolithophore community structure across the subtropical frontal zone in the South Atlantic Ocean. Mar. Micropaleontol. 76, 255–273.

Boeckel, B., Baumann, K.-H., Henrich, R., Kinkel, H., 2006. Coccolith distribution patterns in South Atlantic and Southern Ocean surface sediments in relation to environmental gradients. Deep-Sea Res. Pt. I 53, 1073–1099.

Bopp, L., Resplandy, L., Orr, J.C., Doney, S.C., Dunne, J.P., Gehlen, M., Halloran, P., Heinze, C., Ilyina, T., Séférian, R., Tjiputra, J., Vichi, M., 2013. Multiple stressors of ocean ecosystems in the 21st century: projections with CMIP5 models. Biogeosciences 10, 6225–6245. https://doi.org/10.5194/bg-10-6225-2013.

Bory, A., Jeandel, C., Leblond, N., Vangriesheim, A., Khripounoff, A., Beaufort, L., Rabouille, C., Nicolas, E., Tachikawa, K., Etcheber, H., Buat-Me!nard, P., 2001. Downward particle fluxes within different productivity regimes off the Mauritanian upwelling zone (EUMELI program). Deep-Sea Res. I 48, 2251–2282.

Boyce, D.G., Lewis, M.R., Worm, B., 2010. Global phytoplankton decline over the past century. Nature 466 (29), 591–596.

Boyd, P.W., et al., 2010. Environmental control of open-ocean phytoplankton groups: now and in the future. Limn. Ocean. 55, 1353–1376.

Boyle, E.A., Edmond, J.M., Sholkovitz, E.R., 1977. On the mechanism of iron removal in estuaries. Geoch. Geoph. Acta 41 (1313–1324), 1313–1324.

Brand, L.E., 1994. Physiological ecology of marine coccolithophores. In: Winter, A., Siesser, W.G. (Eds.), Coccolithophores. Cambridge University Press, Cambridge, pp. 39–49.

Broerse, A.T.C., Ziveri, P., van Hinte, J.E., Honjo, S., 2000. Coccolithophore export production, species composition and coccolith- $CaCO_3$ fluxes in the NE Atlantic (34°N 21°W and 48°N 21°W). Deep-Sea Res. Pt. II 47, 1877–1906.

Cermeño, P., Dutkiewicz, S., Harris, R.P., Follows, M., Schofield, O., Falkowski, P.G., 2008. The role of nutricline depth in regulating the ocean carbon cycle. PNAS 105 (51), 20344–20349.

Charalampopoulou, A., Poulton, A.J., Tyrrell, T., Lucas, M.I., 2011. Irradiance and pH affect coccolithophore community composition on a transect between the North Sea and the Arctic Ocean. Mar. Ecol. Prog. Ser. 431, 25–43.

Chavez, F.P., Messié, M., Pennington, J.T., 2011. Marine Primary Production in Relation to Climate Variability and Change. Annu. Rev. Mar. Sci. 3, 227–260.

Chiapello, I., Prospero, J.M., Herman, J.R., Hsu, N.C., 1999. Detection of mineral dust over the North Atlantic Ocean and Africa with the Nimbus 7 TOMS. J. Geophys. Res. 104, 9277–9291.

Cropper, T., Hanna, E., Bigg, G., 2014. Spatial and temporal seasonal trends in coastal upwelling off Northwest Africa, 1981–2012. Deep-Sea Research I 86, 94–111.

Cros, L., 2001. Planktonic coccolithophores of the NW Mediterranean. PhD Thesis. Universitat de Barcelona, pp. 181pp.

Cros, L., Estrada, M., 2013. Holo-heterococcolithophore life cycles: ecological implications. Mar Ecol Progr Ser. 492, 57–68. https://doi.org/10.3354/meps10473.

Cros, L., Fortuño, J.-M., 2002. Atlas of northwestern Mediterranean coccolithophores. Sci. Mar. 66, 7–182.

Dadou, I., Garcon, V., Andersen, V., Flierl, G.R., Davis, C.S., 1996. Impact of the North Equatorial Current relationship to surface hydrography. Deep-Sea Res. 33, 225–246.

De Master, D.J., Kuehl, S.A., Nittrouer, C.A., 1986. Effects of suspended sediments on geochemical processes near the mouth of the Amazon River: examination of biogenic silica uptake and the fate of particle-reactive elements. Cont. Shelf Res. 6, 107–125.

Demarcq, H., 2009. Trends in primary production, sea surface temperature and wind in upwelling systems (1998–2007). Prog. Oceanogr. 83 (1), 376–385.

Dimiza, M.D., Triantaphyllou, M.V., Dermitzakis, M.D., 2008. Seasonality and ecology of living coccolithophores in E. Mediterranean coastal environments (Andros Island, Middle Aegean Sea). Micropaleontology 54 (1), 59–75.

Drinkwater, K.F., Belgrano, A., Borja, A., Conversi, A., Edwards, M., Greene, C.H., Ottersen, G., Pershing, A.J., Walker, H., 2003. The response of marine ecosystems to climate variability associated with the North Atlantic Oscillation. In: In The North Atlantic Oscillation: Climatic Significance and Environmental Impact. Geophysical Monograph 134 American Geophysical Union. https://doi.org/10.1029/134GM10.

Emery, W.J., Meincke, J., 1986. Global water masses: summary and review. Oceanol. Acta 9, 383–391.

Falkowski, P.G., Oliver, M.J., 2007. Mix and match: how climate selects phytoplankton. Nature 5, 813–819.

Falkowski, P.G., Fenchel, T., Delong, E.F., 2008. The microbial engines that drive Earth's biogeochemical cycles. Science 320, 1034–1039.

Fallet, U., van Assen, C., Boer, W., Greaves, M., Brummer, G.-J.A., 2009. A novel application of wet-oxidation to retrieve carbonates from large organic-rich samples for ocean. Clim. Res., Geochem. Geophys. Geosyst. 10, Q08004. https://doi.org/10.1029/2009GC002573.

Ffield, A., 2005. North Brazil current rings viewed by TRMM Microwave Imager SST and the influence of the Amazon Plume. Deep-Sea Res. Pt. I 52, 137–160.

Fischer, G., Reuter, C., Karakas, G., Nowald, N., Wefer, G., 2009a. Offshore advection of particles within the Cape Blanc filament, Mauritania: Results from observational and modelling studies. Prog. Oceanogr. 83, 322–330.

Fischer, G., Karakas, G., Blaas, M., Ratmeyer, V., Nowald, N., Schlitzer, R., Helmke, P., Davenport, R., Donner, B., Neuer, S., Wefer, G., 2009b. Mineral ballast and particle settling rates in the coastal upwelling system off NW Africa and the South Atlantic. Int. J. Earth Sci. 98, 281–298.

Fischer, G., Romero, O., Merkel, U., Donner, B., Iversen, M., Nowald, N., Ratmeyer, V., Ruhland, G., Klann, M., Wefer, G., 2016. Deep ocean mass fluxes in the coastal upwelling off Mauritania from 1988 to 2012: variability on seasonal to decadal timescales. Biogeosciences 13, 3071–3090. https://doi.org/10.5194/bg-13-3071-2016.

Fischer, G., Basse, A., Baumann, K.-H., Klann, M., Klawonn, I., Küchler, R., Nowald, N., Ruhland, G., 2012. Report and preliminary results of RV POSEIDON Cruise P425. Las Palmas – Las Palmas, 16.01.2012 – 30.01.2012. Berichte, Fachbereich Geowissenschaften, Universität Bremen, No. 287, 32 pages. Bremen, 2012.

Fischer, G., M. Ba, K. Dehning, J. Hefter, M. Iversen, M. Klann, N. Nowald, H. Ploug, G. Ruhland, Y. Witte, 2013. Report and preliminary results of R/V POSEIDON cruise POS445. Las Palmas – Las Palmas, 19.01.2013 – 01.02.2013. Berichte, MARUM – Zentrum für Marine Umweltwissenschaften, Fachbereich Geowissenschaften, Universität Bremen, No. 298, 30 pages. Bremen, 2013. ISSN 2195-9633.

Fischer, G., Dehning, K., Dia, A., Füssel, J., Hefter, J., Iversen, M., Klann, M., Nowald, N., Olbrich, M., Ruhland, G., 2014. Report and preliminary results of R/V POSEIDON cruise POS464, Las Palmas (Canary Islands) – Las Palmas (Canary Islands), 03.02. 2014 – 18.02.2014. Berichte, MARUM – Zentrum für Marine Umweltwissenschaften, Fachbereich Geowissenschaften, Universität Bremen, No. 304, 29 pages. Bremen, 2014. ISSN 2195-7894.

Gabric, A.J., Garcia, L., Van Camp, L., Nykjaer, L., Eifler, W., Schrimpf, W., 1993. Offshore export of shelf production in the Cape Blanc (Mauritania) giant filament as derived from coastal zone color scanner imagery. J. Geophys. Res. 98 (C3), 4697–4712.

Garcia, H.E., Locarnini, R.A., Boyer, T.P., Antonov, J.I., Baranova, O.K., Zweng, M.M., Reagan, J.R., Johnson, D.R., 2014. World Ocean Atlas 2013, Volume 4: Dissolved Inorganic Nutrients (phosphate, nitrate, silicate). In: In: Levitus, S., Mishonov, A. (Eds.), NOAA Atlas NESDIS 76 25 pp.

García-Reyes, M., Sydeman, W.J., Schoeman, D.S., Rykaczewski, R.R., Black, B.A., Smit, A.J., Bograd, S.J., 2015. Under pressure: climate change, upwelling, and eastern boundary upwelling ecosystems. Front. Mar. Sci. 2, 109. https://doi.org/10.3389/fmars.2015.00109.

Garzoli, S., Katz, E.J., 1983. The forced reversal of the Atlantic North equatorial countercurrent. J. Phys. Oceanogr. 13, 2082–2090.

George, S.E., Saunders, M.A., 2001. North Atlantic Oscillation impact on tropical north Atlantic winter atmospheric variability. Geophys. Res. Lett. 28 (6), 1015–1018.

Gómez-Gesteira, M., De Castro, M., Álvarez, I., Lorenzo, M.N., Gesteira, J.L.G., Crespo, A.J.C., 2008. Spatio-temporal upwelling trends along the Canary Upwelling System (1967–2006). Ann. N. Y. Acad. Sci. 1146 (1), 320–337.

Gregg, W., Rousseaux, C., 2017. NASA Ocean Biogeochemical Model assimilating satellite chlorophyll data global daily VR2017, Edited by Watson Gregg and Cecile Rousseaux, Greenbelt, MD, USA, Goddard Earth Sciences Data and Information Services Center (GES DISC), Accessed: June 2019, 10.5067/PT6TXZKSHBW9.

Guerreiro, C.V., Baumann, K.-H., Brummer, G.-J.A., Fischer, G., Korte, L.F., Merkel, U.S.C., de Stigter, H., Stuut, J.-B.W., 2017. Coccolithophore fluxes in the open tropical North Atlantic: influence of thermocline depth, Amazon water, and Saharan dust. Biogeosciences 14, 4577–4599. https://doi.org/10.5194/bg-14-4577-2017.

Guerreiro, C., Oliveira, A., Cachão, M., de Stigter, H., Sá, C., Borges, C., Cros, C., Santos, A., Rodrigues, A., 2013. Late winter coccolithophore bloom off central Portugal in response to river discharge and upwelling. Cont. Shelf Res. 59, 65–83.

Guerreiro, C., De Stigter, H., Cachão, M., Oliveira, A., Rodrigues, A., 2015. Coccoliths from recent sediments of the Central Portuguese Margin: taphonomical and ecological inferences. Mar. Micropaleontol. 114, 55–68.

Hagino, K., Bendif, E.M., Probert, I., Young, J., 2017. Molecular phylogenetic position of Reticulofenestra sessilis. In: Proceedings of the 16th INA, Athens, Greece.

Haidar, A.T., Thierstein, H.R., 2001. Coccolithophore dynamics off Bermuda (N. Atlantic). Deep-Sea Res. Pt. II 48, 1925–1956.

Hoegh-Guldberg, O., Cai, R., Poloczanska, E.S., Brewer, P.G., Sundby, S., Hilmi, K., Fabry, V.J., Jung, S., 2014. The Ocean. In: Barros, V.R., Field, C.B., Dokken, D.J., Mastrandrea, M.D., Mach, K.J., Bilir, T.E., Chatterjee, M., Ebi, K.L., Estrada, Y.O., Genova, R.C., Girma, B., Kissel, E.S., Levy, A.N., MacCracken, S., Mastrandrea, P.R., White, L.L. (Eds.), Climate Change 2014: Impacts, Adaptation, and Vulnerability. Part B: Regional Aspects. Contribution of Working Group II to the Fifth Assessment Report of the Intergovernmental Panel on Climate Change. Cambridge University Press, Cambridge, United Kingdom and New York, NY, USA, pp. 1655–1731.

Holte, J., Talley, L.D., Gilson, J., Roemmich, D., 2017. An Argo mixed layer climatology and database. Geophys. Res. Lett. 44, 5618–5626. https://doi.org/10.1002/2017GL073426.

Houdan, A., Billard, C., Marie, D., Not, F., Sá, A., Young, J., Probert, I., 2006. Holococcolithophore- heterococcolithophore (Haptophyta) life cycles: flow cytometric analysis of relative ploidy levels. Syst. Biodivers. 1 (4), 453–465. https://doi.org/10.1017/S1477200003001270.

Hurrell, J.H., Kushnir, Y., Ottersen, G., Visbeck, M., 2003. An overview of the North Atlantic Oscillation. In: The North Atlantic Oscillation: Climatic Significance and Environmental Impact. Geophysical Monograph 134 American Geophysical Union. https://doi.org/10.1029/134GM01.

Irwin, A.J., Finkel, Z.V., Müller-Karger, F.E., Ghinaglia, L.T., 2015. Phytoplankton adapt to changing ocean environments. PNAS 112 (18), 5762–5766.

Johns, W., Lee, T., Beardsley, R.C., Candela, J., Limeburner, R., Castro, B., 2004. Annual cycle and variability of the North Brazil Current. J. Phys. Oceanogr. 28, 103–128.

Jordan, R., Cros, L., Young, J., 2004. A revised classification scheme for living haptophytes. Micropaleontol. 50, 55–79.

Karl, D., Letelier, R., Tupas, L., Dore, J., Christian, J., Hebel, R., 1997. The role of nitrogen fixation in the biogeochemical cycling in the subtropical North Pacific Ocean. Nature 388, 533–538.

Katz, E.J., 1981. Dynamic topography of the sea surface in the equatorial Atlantic. J. Mar. Res. 39, 53–63.

Katz, M.E., Finkel, Z.V., Grzebyk, D., Knoll, A.H., Falkowski, P.G., 2004. Evolutionary trajectories and biogeochemical impacts of marine eukaryotic phytoplankton. Annu. Rev. Ecol. Evol. Syst. 35, 523–556.

Kinkel, H., Baumann, K.-H., Cepek, M., 2000. Coccolithophores in the equatorial Atlantic Ocean: response to seasonal and Late Quaternary surface water variability. Mar. Micropaleontol. 39, 87–112.

Kleijne, A., 1991. Holococcolithophorids from the Indian Ocean, Red Sea, Mediterranean Sea and North Atlantic Ocean. Mar Micropaleontol. 17 (1–2), 1–76.

Kleijne, A., Jordan, R.W., Heimdal, B.R., Samtleben, C., Chamberlain, A.H.L., Cros, L., 2002. Five new species of the coccolithophorid genus Alisphaera (Haptophyta), with notes on their distribution, cocco1ith structure and taxonomy. Phycologia 40, 583–601.

Knappertsbusch, M., 1993. Geographic distribution ofliving and Holocene coccolithophorids in the Mediterranean Sea. Mar. Micropaleontol. 21, 219–247.

Knappertsbusch, M., Brummer, G.-J.A., 1995. A sediment trap investigation of sinking coccolithophores in the North Atlantic, Deep-Sea Res. I 42, 1083–1109.

Köbrich, M.I., Baumann, K.-H., 2009. Coccolithophore flux in a sediment trap off Cape Blanc (NW Africa). J. Nannoplankton Res. 30, 83–96.

Köbrich, M.I., Baumann, K.-H., Fischer, G., 2015. Seasonal and inter-annual dynamics of coccolithophore fluxes from the up- welling region off Cape Blanc, NW Africa. J. Micropalaeontol. 35, 103–116. https://doi.org/10.1144/jmpaleo2014-024.

Korte, L.F., Brummer, G.-J.A., van der Does, M., Guerreiro, C.V., Hennekam, R., van Hateren, J.A., Jong, D., Munday, C.I., Schouten, S., Stuut, J.-B.W., 2017. Downward particle fluxes of biogenic matter and Saharan dust across the equatorial North Atlantic. Atmos. Chem. Phys. 17, 6023–6040. https://doi.org/10.5194/acp-17-6023-2017.

Krumhardt, K.M., Lovenduski, N.S., Freeman, N.M., Bates, N.R., 2016. Apparent increase in coccolithophore abundance in the subtropical North Atlantic from 1990 to 2014. Biogeosciences 13, 1163–1177. https://doi.org/10.5194/bg-13-1163-2016.

Krumhardt, K.M., Lovenduski, N.S., Long, M.C., Lindsay, K., 2017. Avoidable impacts of ocean warming on marine primary production: Insights from the CESM ensembles. Global Biogeochem. Cycl. 31, 114–133. https://doi.org/10.1002/2016GB005528.

Lancelot, C., 2012. Marine nutrient cycling – how will the ocean's capacity of biological carbon pumping change? PAGES News 20 (1), 16.

Lathuilière, C., Echevin, V., Levy, M., 2008. Seasonal and intraseasonal surface chlorophyll-a variability along the northwest African coast. J. Geophys. Res. Ocean. 13, C05007. https://doi.org/10.1029/2007JC004433.

Laufkoetter, C., Vogt, M., Gruber, N., 2013. Trends in marine plankton composition and export production in a CCSM-BEC hindcast (1960–2006). EGU General Assembly Conference Abstracts, Vienna, Austria.

Levitus, S., 1982. Climatological atlas of the world ocean. NOAA Prof. Paper 13, 173.

Li, H., Xu, F., Zhou, W., Wang, D., Wright, J.S., Liu, Z., Lin, Y., 2017. Development of a global gridded Argo data set with Barnes successive corrections. J. Geophys. Res. Oceans 122. https://doi.org/10.1002/2016JC012285.6.

Locarnini, R.A., Mishonov, A.V., Antonov, J.I., Boyer, T.P., Garcia, H.E., Baranova, O.K., Zweng, M.M., Paver, C.R., Reagan, J.R., Johnson, D.R., Hamilton, M., Seidov, D., 2013. World Ocean Atlas 2013, Volume 1: Temperature. In: In: Levitus, S., Mishonov, A. (Eds.), NOAA Atlas NESDIS 73 40 pp.

Longhurst, A., 1993. Seasonal cooling and blooming in tropical oceans. Deep-Sea Res. I 40, 2145–2165.

Lozier, M.S., Dave, A.C., Palter, J.B., Gerber, L.M., Barber, R.T., 2011. On the relationship between stratification and primary productivity in the North Atlantic. Geophys. Res. Lett. 38, L18609. https://doi.org/10.1029/2011GL049414.

Mann, K.H., Lazier, J.R., 2006. Dynamics of Marine Ecosystems, Biological-Physical Interactions in the Oceans, third ed. Black-well Publishing, Malden, MA, Oxford, UK, pp. 512.

Margalef, R., 1978. Life-forms of phytoplankton as survival alternatives in an unstable environment. Oceanol. Acta 1, 493–509.

McClain, C.R., Firestone, J., 1993. An investigation of Ekman upwelling in the North Atlantic. J. Geophys.Res. 98, 12327–12339.

McGillicuddy, D.J., Robinson, A.R., Siegel, D.A., Jannasch, H.W., Johnson, R., et al., 1998. Influence of mesoscale eddies on new production in the Sargasso Sea. Nature 394, 263–266.

McGregor, H.V., Dima, M., Fischer, H.W., Mulitza, S., 2007. Rapid 20th-Century Increase in Coastal Upwelling off Northwest Africa. Science 315, 637–639.

McMahon, K.W., et al., 2015. Millennial- scale plankton regime shifts in the subtropical North Pacific Ocean. Science 350 (6267), 1530–1532.

Merle, J., 1980a. Seasonal heat budget in the equatorial Atlantic Ocean. J. Phys. Oceanogr. 10, 464–469.

Merle, J., 1980b. Seasonal variation of heat storage in the tropical Atlantic Ocean. Oceanol. Acta 3, 455463.

Molfino, B., McIntyre, A., 1990. Precessional forcing of nutricline dy- namics in the equatorial Atlantic. Science 249, 766–769.

Molleri, G.S.F., Novo, E.M.L., Kampel, M., 2010. Space–time variability of the Amazon River plume based on satellite ocean color. Cont. Shelf Res. 30, 342–352.

Moore, J.K., Fu, W., Primeau, F., Britten, G.L., Lindsay, K., Long, M., Doney, S.C., Mahowald, N., Hoffman, F., Randerson, J.T., 2018. Sustained climate warming drives declining marine biological productivity. Science 359, 1139–1143.

Morán, X.A.G., López-Urrutia, A., Calvo-Díaz, A., Li, W.K.W., 2010. Increasing importance of small phytoplankton in a warmer ocean. Glob. Change Biol. 16, 1137–1144.

Morel, A., 1996. An ocean flux study in eutrophic, mesotrophic and oligotrophic situations: The EUMELI program. Deep-Sea Res. I 43 (8), 1185–1190.

Morel, A., 2000. Process studies in eutrophic, mesotrophic, and oligotrophic oceanic regimes within the tropical northeast Atlantic. In: Hanson, R.B., Duclow, H.W., Field, J.F. (Eds.), The Changing Ocean Carbon Cycles. Cambridge University Press, Cambridge, pp. 338–374.

Müller, A.H., 1963. Lehrbuch de Paläozoologie, Band 1. Allgemeine Grundlagen. Gustav Fischer Verlag, Jena 387p.

Muller-Karger, F., McClain, C., Richardson, P., 1988. The dispersal of the Amazon's water. Nature 333, 56–58.

Narciso, A., Gallo, F., Valente, A., Cachão, M., Cros, L., Azevedo, E.D., Barcelos e Ramos, J., 2016. Seasonal and interannual variations in coccolithophore abundance off Terceira Island, Azores (Central North Atlantic). Continent. Shelf Res. 117 (2016), 43–56.

O'Brien, C.J., Vogt, M., Gruber, N., 2016. Global coccolithophore diversity: drivers and future change. Prog. Oceanogr. 140, 27–42.

Okada, H., Honjo, S., 1973. The distribution of oceanic coccolithophorids in the Pacific. Deep-Sea Res. 20, 355–374.

Oschlies, A., Garçon, V., 1998. Eddy-induced enhancement of primary production in a coupled ecosystem-circulation model of the North Atlantic Ocean. Nature 394, 266–269.

Oschlies, A., 2002. Nutrient supply to the surface waters of the North Atlantic: A model study. J. Geophys. Res. 107 (C5), 3046. https://doi.org/10.1029/2000JC000275.

Ottens, J., Nederbragt, A., 1992. Planktic foraminiferal diversity as indicator of ocean environments. Mar. Micropaleontol. 19 (1–2), 13–28.

Pastor, M.V., Palter, J.B., Pelegrí, J.L., Dunne, J.P., 2013. Physical drivers of interannual chlorophyll variability in the eastern subtropical North Atlantic. J Geophys Res Oceans 118, 3871–3886.

Pastor, M.V., Pelegrí, J.L., Hernández-Guerra, A., Font, J., Salat, J., Emelianov, M., 2008. Water and nutrient fluxes off northwest Africa. Cont. Shelf Res. 28, 915–936.

Pastor, M.V., Peña-Izquierdo, J., Pelegrí, J.L., Marrero-Díaz, A., 2012. Meridional changes in water mass distributions off NW Africa during November 2007/2008. Cienc. Mar. 38 (1B), 223–244.

Pelegrí, J.L., Peña-Izquierdo, J., Machín, F., Meiners, C., Presas-Navarro, C., 2017. Oceanography of the Cape Verde Basin and Mauritanian Slope Waters. In: Ramos, A., Ramil, F., Sanz, J. (Eds.), Deep-Sea Ecosystems Off Mauritania, Research of Marine Biodiversity and Habitats in the Northwest African Margin, pp. 119–153.

Philander, S.G., 2001. Atlantic Ocean Equatorial Currents. Encyclop. Ocean Sci. 188–191. https://doi.org/10.1006/rwos.2001.0361.

Piontkovski, S.A., O'Brien, T.D., Umani, S.F., Krupa, E.G., Stuge, T.S., Balymbetov, K.S., Grishaeva, O.V., Kasymov, A.G., 2006. Zooplankton and the North Atlantic Oscillation: a basin-scale analysis. J. Plankton Res. 28 (11), 1039–1046.

Polovina, J.J., Howell, E.A., Abecassis, M., 2008. Ocean's least productive waters are expanding. Geophys. Res. Lett. 35, L03618.

Poulton, A.J., Holligan, P.M., Charalampopoulou, A., Adey, T.R., 2017. Coccolithophore ecology in the tropical and subtropical Atlantic Ocean: new perspectives from the Atlantic Meridional Transect (AMT) programme. Prog. Oceanogr. https://doi.org/10.1016/j.pocean.2017.01.003.

Ratmeyer, V., Fischer, G., Wefer, G., 1999. Lithogenic particle fluxes and grain size distributions in the deep ocean off northwest Africa: Implications for seasonal changes of eolian dust input and downward transport. Deep Sea Res. Part I 46, 1289–1337.

Reid, J.L., 1994. On the total geostrophic circulation of the North Atlantic Ocean: flow patterns, tracers, and transports. Prog. Oceanogr. 33, 1–92.

Richardson, P.L., Walsh, D., 1986. Mapping climatological seasonal variations of surface currents in the tropical Atlantic using ship drifts. J. Geophys. Res. 91, 10537–10550.

Rivero-Calle, S., Gnanadesikan, A., Del Castillo, C.E., Balch, W.M., Guikema, S.D., 2015. Multidecadal increase in North Atlantic coccolithophores and the potential role of rising CO_2. Science 350 (6267), 1533–1537.

Romero, O.E., Dupont, L., Wyputta, U., Jahns, S., Wefer, G., 2003. Temporal variability of fluxes of eolian-transported freshwater diatoms, phytoliths, and pollen grains off Cape Blanc as reflection of land-atmosphere-ocean interactions in northwest Africa. J. Gephys. Res. 108 (C5), 3153. https://doi.org/10.1029/2000JC000375.

Rost, B., Riebesell, U., 2004. Coccolithophores and the biological pump: responses to environmental changes. In: Thierstein, H.R., Young, J.R. (Eds.), Coccolithophores: From Molecular Processes to Global Impact. Springer, Berlin, pp. 99–125.

Rumyantseva, A., Lucas, N., Rippeth, T., Martin, A., Painter, S.C., Boyd, T.J., Henson, S., 2015. Ocean nutrient pathways associated with the passage of a storm. Global Biogeochem. Cycl. 29, 1179–1189. https://doi.org/10.1002/2015GB005097.

Scheuvens, D., Schütz, L., Kandler, K., Ebert, M., Weinbruch, S., 2013. Bulk composition of northern African dust and its source sediments—a compilation. Earth Sci. Rev. 116, 170–194.

Schuetz, L., 1980. Long range transport of desert dust with special emphasis on the Sahara, in Aerosols: Anthropogenic and natural, sources and transport, edited by T. J. Kneip and P. J. Lioy. Ann. N. Y. Acad. Sci. 338, 515–532.

Siedler, G., Zangenberg, N., Onken, R., Morliere, A., 1992. Seasonal changes in the tropical Atlantic circulation: observations and simulations of the Guinea Dome. J. Geophys. Res. 97, 703–715.

Signorini, S.R., McClain, C.R., 2012. Subtropical gyre variability as seen from satellites. Remote Sens. Lett. 3 (6), 471–479.

Signorini, S.R., Franz, B.A., McClain, C.R., 2015. Chlorophyll variability in the oligotrophic gyres: mechanisms, seasonality and trends. Front. Mar. Sci. 2 (1) 11 pp.

Sprengel, C., Baumann, K.-H., Henderiks, J., Henrich, R., Neuer, S., 2002. Modern coccolithophore and carbonate sedimentation along a productivity gradient in the Canary Islands region: seasonal export production and surface accumulation rates. Deep-Sea Res. II 49, 3577–3598.

Stoll, H.M., Arevalos, A., Burke, A., Ziveri, P., Mortyn, G., Shimizu, N., Unger, D., 2007. Seasonal cycles in biogenic pro- duction and export in Northern Bay of Bengal sediment traps. Deep-Sea Res. II 54, 558–580.

Stramma, L., England, M., 1999. On the water masses and mean circulation of the South Atlantic Ocean. J. Geophys. Res. 104, 20863–20883.

Stuut, J.-B.W., Brummer, G.-J., van der Does, M., Friese, C., Geerken, E., van der Heide, R., Korte, L., Koster, B., Metcalfe, B., Munday, C., van Ooijen, J., Siccha, M., Veldhuizen, R., de Visser, J.-D., Witte, Y., Wuis, L., 2013. Cruise report and preliminary results (64PE378), TRAFFIC II: Transatlantic fluxes of Saharan dust (Las Palmas de Gran Canaria, Spain – St. Maarten). Royal NIOZ, the Netherlands 54 pp.

Sunagawa, S., et al., 2015. Structure and function of the global ocean microbiome. Science 348 (6237), 1261359–1261361.

Sydeman, W.J., García-Reyes, M., Schoeman, D., Rykaczewski, R.R., Thompson, S.A., Black, B.A., et al., 2014. Climate change and wind intensification in coastal upwelling ecosystems. Science 345, 77–80. https://doi.org/10.1126/science.1251635.

Thomas, A., Strub, P., Carr, M.-E., Weatherbee, R., 2004. Comparisons of chlorophyll variability between the four major global eastern boundary currents. Int. J. Remote Sens. 25 (7–8), 1443–1447.

Thomas, M.K., Kremer, Colin T., Klausmeier, Christopher A., Litchman, Elena, 2012. A global pattern of thermal adaptation in marine phytoplankton. Science 338, 1085. https://doi.org/10.1126/science.1224836.

Triantaphyllou, M.V., Dermitzakis, M.D., Dimiza, M.D., 2002. Holo- and heterococcolithophorids (calcareous nannoplankton) in the gulf of Korthi (Andros Island, Aegean Sea, Greece) during late summer 2001. Rev. Paleobiol. 21 (1), 353–369.

Triantaphyllou, M.V., Baumann, K.-H., Karatsolis, B.-T., Dimiza, M.D., Psarra, S., Skampa, E., Patoucheas, P., Vollmar, N., Koukousioura, O., Katsigera, A., Krasakopoulou, E., Nomikou, P., 2018. Coccolithophore community response along a natural CO2

gradient off Methana (SW Saronikos Gulf, Greece, NE Mediterranean). PLoS ONE 13 (7), e0200012. https://doi.org/10.1371/journal.pone.0200012.
Tuomisto, H., 2013. Defining, measuring, and partitioning species diversity. Encycloped. Biodivers. 2, 434–446. https://doi.org/10.1016/B978-0-12-384719-5.00378-6.
Van Camp, L., Nykjær, L., Mittelstaedt, E., Schlittenhardt, P., 1991. Upwelling and boundary circulation off Northwest Africa as depicted by infrared and visible satellite observations. Prog. Oceanogr. 26, 357–402.
van der Jagt, H., Friese, C., Stuut, J.-B.W., Fischer, G., Iversen, M.H., 2018. The ballasting effect of Saharan dust deposition on aggregate dynamics and carbon export: aggregation, settling, and scavenging potential of marine snow. Limnol. Oceanogr. 1–9. https://doi.org/10.1002/lno.10779.
Varona, H.L., Veleda, D., Silva, M., Cintra, M., Araujo, M., 2019. Amazon river plume influence on western tropical Atlantic dynamic variability. Dyn. Atmos. Oceans 85, 1–15.
Visbeck, M., Chassignet, E.P., Curry, R., Delworth, T., Dickson, B., Krahmann, G., 2003. The Ocean's response to North Atlantic oscillation variability. The North Atlantic Oscillation: Climatic Significance and Environmental Impact. Geophysical Monograph Series 134.
Waniek, J., Koeve, W., Prien, R.D., 2000. Trajectories of sinking particles and the catchment areas above sediment traps in the northeast Atlantic. J. Mar. Res. 58, 983–1006.
Winter, A., Siesser, W.G., 1994. Atlas of living coccolithophores. In: Winter, A., Siesser, W.G. (Eds.), Coccolithophores. Cambridge University Press, Cambridge, pp. 107–159.
Winter, A., Jordan, R., Roth, P., 1994. Biogeography of living coccolithophores in ocean waters. In: Winter, A., Siesser, W. (Eds.), Coccolithophores. Cambridge Univ. Press, pp. 161–177.
Winter, A., Rost, B., Hilbrecht, H., Elbrachter, M., 2002. Vertical and horizontal distribution of coccolithophores in the Caribbean Sea. Geo-Mar. Lett. 22, 150–161.
Winter, A., Henderiks, J., Beaufort, L., Rickaby, R., Brown, C., 2013. Poleward expansion of the coccolithophore Emiliania huxleyi. J. Plankton Res. 1–10. https://doi.org/10.1093/plankt/fbt110.
Yang, T.-N., Wei, K.-Y., 2003. How many coccoliths are there in a coccosphere of the extant coccolithophorids? A compilation. J. Nannoplankton Res. 25 (I), 7–15.
Young, J.R., Bown, P.R., Lees, J.A. (Eds.), 2011. Nannotax Website. International Nannoplankton Association. http://www.mikrotax. org/Nannotax3/ (last access: 21 September 2011).
Young, J.R., Geisen, M., Cros, L., Kleijne, A., Probert, I., Ostergaard, J.B., 2003. A guide to extant coccolithophore taxonomy. J. Nannoplankton Res. Spec. Iss. 1, 1–132.
Young, J., 1994. Functions of coccoliths. Cambridge Univ. Press, Cambridge, pp. 63–82.
Zenk, W., Klein, B., Schroder, M., 1991. Cape Verde frontal zone. Deep-Sea Res. Pt. I 38, 505–530.
Ziveri, P., Baumann, K.-H., Boeckel, B., Bollmann, J., Young, J.R., 2004. Biogeography of selected Holocene coccoliths in the Atlantic Ocean. In: Thierstein, H.R., Young, J.R. (Eds.), Coccolithophores – From Molecular Processes to Global Impact. Springer, Berlin, pp. 403–428.
Ziveri, P., de Bernardi, B., Baumann, K.-H., Stoll, H.M., Mortyn, P.G., 2007. Sinking of coccolith carbonate and potential contribution to organic carbon ballasting in the deep ocean. Deep-Sea Res. II 54, 659–675.
Shaolei, L., Hong, L., Jianping, X., Zenghong, L., Xiaofen, W., Chaohui, S., Minjie. C., 2018. Manual of Global Ocean Argo gridded data set (BOA_Argo) (Version 2018), 13 pp.